



Tropospheric NO₂
columns over East
Asia

K. M. Han et al.

This discussion paper is/has been under review for the journal Atmospheric Chemistry and Physics (ACP). Please refer to the corresponding final paper in ACP if available.

Evaluating the accuracy of NO_x emission fluxes over East Asia by comparison between CMAQ-simulated and OMI-retrieved NO₂ columns with the application of averaging kernels from the KNMI algorithm

K. M. Han^{1,2}, S. Lee^{1,2}, I. S. Chang³, and C. H. Song^{1,2}

¹School of Environmental Science and Engineering, Gwangju Institute of Science and Technology (GIST), Gwangju, 500-712, Korea

²Advanced Environmental Monitoring Research Center (ADEMRC), Gwangju Institute of Science and Technology (GIST), Gwangju, 500-712, Korea

³Air Quality Research Division, National Institute of Environmental Research (NIER), Incheon, 404-708, Korea

Title Page

Abstract

Introduction

Conclusions

References

Tables

Figures



Back

Close

Full Screen / Esc

Printer-friendly Version

Interactive Discussion



Received: 17 June 2014 – Accepted: 20 June 2014 – Published: 30 June 2014

Correspondence to: C. H. Song (chsong@gist.ac.kr)

Published by Copernicus Publications on behalf of the European Geosciences Union.

ACPD

14, 17585–17634, 2014

Tropospheric NO₂ columns over East Asia

K. M. Han et al.

Title Page

Abstract

Introduction

Conclusions

References

Tables

Figures



Back

Close

Full Screen / Esc

Printer-friendly Version

Interactive Discussion



Abstract

To evaluate the accuracy of bottom-up NO_x emissions in East Asia, CMAQ-calculated NO₂ columns were compared with OMI-retrieved NO₂ columns. For a direct comparison between the two NO₂ columns, the averaging kernels (AKs) retrieved from the Royal Netherlands Meteorological Institute (KNMI) algorithm were applied to the CMAQ model simulations. When the two NO₂ columns before and after the applications of AKs were compared over East Asia, it was found that, for example, the normalized mean errors (NMEs) between the CMAQ-estimated and OMI-retrieved NO₂ columns were reduced significantly, from ~ 103 % to ~ 46 %, from ~ 112 % to ~ 45 %, and from ~ 135 % to ~ 40 % during spring, fall, and winter, respectively. Also, the two tropospheric NO₂ columns were better correlated spatially in East Asia ($R = 0.71\text{--}0.94$) after the application of the AKs. From this study, it was found that the NO_x emissions used were, on annual average, ~ 28 % underestimated in East Asia, although some overestimates were also found, partly over southern Central East China, the Sichuan Basin, and South Korea regions during the winter. However, these results can also be influenced by several uncertainty factors in the CMAQ model simulations, such as monthly variation and the strength of the NO_x emissions. Thus, we also applied different monthly variation and different strengths of the NO_x emissions to the CMAQ model simulations over East Asia. The results showed strong impacts on the tropospheric NO₂ columns in East Asia, indicating that these two factors are also important. Further sensitivity analysis was conducted with reaction probabilities of N₂O₅ onto atmospheric aerosols. Those results are also discussed in detail in this manuscript. Although several uncertainty factors are discussed, it was concluded that the consideration of the AKs is the single most important factor in investigating the accuracy of bottom-up NO_x emissions generally being used in CTM simulations.

Tropospheric NO₂ columns over East Asia

K. M. Han et al.

Title Page

Abstract

Introduction

Conclusions

References

Tables

Figures



Back

Close

Full Screen / Esc

Printer-friendly Version

Interactive Discussion



1 Introduction

There has been growing public concern about serious smog events in East Asia due to large amounts of anthropogenic pollutants in the atmosphere. Among the pollutants, nitrogen oxides ($\text{NO}_x = \text{NO} + \text{NO}_2$) play a key role in tropospheric chemistry, such as ozone and secondary aerosol formation. Also, in global climate change, atmospheric NO_x is believed to make indirect negative contributions to radiative forcing in the atmosphere (Wild et al., 2001). For example, secondary nitrates (NO_3^-) formed via the condensation of atmospheric HNO_3 , NO_3 , and N_2O_5 into particles contribute, on average, 30.7 % to aerosol direct radiative forcing (ADRF) in East Asia during the winter season, which cannot be ignored in the estimation of direct radiative forcing in East Asian (Park et al., 2014). HNO_3 formation via the reaction of $\text{OH} + \text{NO}_2$ during the daytime and heterogeneous nitrate formation via the condensation of N_2O_5 onto atmospheric particles during the nighttime are believed to be the main chemical and physico-chemical processes removing NO_x from the atmosphere (Han and Song, 2012).

Recently, several studies have reported annual increases in NO_x emissions in China (Zhang et al., 2007, 2009; Kurokawa et al., 2013). For example, based on the Greenhouse gas and Air pollution INTERactions and Synergies (GAINS) model simulations, China makes the largest contribution to global NO_x emissions, and its contribution was estimated to be 25 % for 2010 (Cofala et al., 2012). Also, when several emissions scenarios are applied to future GAINS simulations, the contribution of China is estimated to increase, to ~ 29 % in the years between 2015 and 2035 (Cofala et al., 2012). However, large uncertainty in bottom-up NO_x emissions over East Asia has also been reported (e.g. Streets et al., 2003; Zhang et al., 2007; Klimont et al., 2009; Xing et al., 2011).

In the meantime, several studies have also reported rapid increases in atmospheric NO_x mixing ratios over China, based on Global Ozone Monitoring Experiment (GOME), Ozone Monitoring Instrument (OMI), and SCanning Imaging Absorption spectroMeter for Atmospheric CartographY (SCIAMACHY) observations (Richter et al., 2005; van der A et al., 2006; Itahashi et al., 2014). These satellite observations have provided

Tropospheric NO_2 columns over East Asia

K. M. Han et al.

Title Page

Abstract

Introduction

Conclusions

References

Tables

Figures



Back

Close

Full Screen / Esc

Printer-friendly Version

Interactive Discussion



Tropospheric NO₂ columns over East Asia

K. M. Han et al.

Title Page

Abstract

Introduction

Conclusions

References

Tables

Figures



Back

Close

Full Screen / Esc

Printer-friendly Version

Interactive Discussion



useful global/regional information on the mixing ratios and spatial distributions of NO_x, and have also been used to investigate the accuracy of the global and regional NO_x emissions (e.g. Martin et al., 2006; Uno et al., 2007; Wang et al., 2007; Han et al., 2009). However, these satellite-retrieved column quantities are not “real” or “true” values, having different vertical sensitivities of the satellite measurements at different altitudes in the atmosphere. To consider this vertical sensitivity of the satellite observations, averaging kernels (AKs) have been introduced into comparison studies between chemistry-transport model (CTM)-simulated and satellite-retrieved NO₂ columns (hereafter, denoted as Ω_{NO_2}) (e.g. Rodgers, 2000; Eskes and Boersma, 2003). In particular, Eskes and Boersma (2003) reported that the use of AKs is crucial in interpreting the retrieved Ω_{NO_2} near the surface, because of the low sensitivity of satellite observations of NO₂ near the surface areas. In this context, several studies have used AKs to evaluate the accuracy of surface NO_x emissions over several regions (e.g. Herron-Thorpe et al., 2010; Lamsal et al., 2010; Ghude et al., 2013).

Evaluating the accuracy of the NO_x emission fluxes in East Asia is also important in more accurately predicting mixing ratios of atmospheric gases and aerosols and estimating DRF by aerosols. The main objective of this study was thus to investigate the accuracy of the bottom-up NO_x emissions in East Asia, comparing OMI-retrieved tropospheric NO₂ columns ($\Omega_{\text{NO}_2,\text{OMI}}$) from KNMI/DOMINO v2.0 daily products with the CTM-calculated NO₂ columns ($\Omega_{\text{NO}_2,\text{CTM}}$). To conduct this investigation, we also applied the AKs retrieved from the KNMI algorithm to the CTM simulations over East Asia for a direct comparison between the CTM-estimated and satellite-observed Ω_{NO_2} in this study (refer to Sect. 3.1).

Precise evaluations of the accuracy of bottom-up NO_x emissions via comparisons between $\Omega_{\text{NO}_2,\text{OMI}}$ and $\Omega_{\text{NO}_2,\text{CTM}}$ are frequently hampered by several uncertainty factors. Thus, another issue in this study was to explore these uncertainty factors, such as uncertainties in monthly variations of NO_x emissions, strength of NO_x emissions, reaction probabilities of N₂O₅ etc. These issues will be discussed further in Sect. 3.2.

2 Experimental methods

The basic approach of this study was to compare the CTM-calculated NO₂ columns with satellite-derived NO₂ columns to investigate the accuracy of bottom-up NO_x emissions in East Asia. Thus, the two major tools (CTM simulations and satellite observations) for this study are described briefly in Sect. 2.

2.1 Modeling descriptions

First, for the CTM simulations, the US EPA/Models-3 CMAQ (Community Multi-scale Air Quality) v4.7.1 model was used (Byun and Schere, 2006). To drive CMAQ model simulations, two main drivers are needed: (i) meteorological fields and (ii) emission fields. For the former, PSU/NCAR MM5 (Pennsylvania state University/National Center for Atmospheric Research Meso-scale Model 5) v3.7.1 was used with National Centers for Environmental Prediction (NCEP) reanalyzed data sets (Stauffer and Seaman, 1990, 1994). To prepare more accurate meteorological fields, four-dimensional data assimilation (FDDA) using QuickSCAT 10 m wind data sets was also carried out. For the latter, three anthropogenic emission inventories were used: INTEX-B (Intercontinental Chemical Transport Experiment-Phase B), CAPSS (Clean Air Policy Support System), and REAS (Regional Emission Inventory in Asia) emission inventories over China, Korea, and Japan, respectively (Ohara et al., 2007; Hong et al., 2008; Zhang et al., 2009). For biogenic emissions, the MEGAN+MOHYCAN (Model of Emissions of Gases and Aerosols from Nature + Model for Hydrocarbon emissions by the CANopy) inventory was obtained from the official website, at <http://tropo.aeronomie.be/models/mohycan.htm> (Müller et al., 2008). Biogenic emissions are an important factor during the summer, even in this type of NO_x study, because the mixing ratios of biogenic species can influence the NO₂-to-NO ratios via changing the levels of HO_x and RO₂ radicals (Horowitz et al., 2007; Han et al., 2009). The accuracy of the biogenic emissions used in this study was also evaluated over the same domain, East Asia, in our previous study (Han et al., 2013).

Title Page

Abstract

Introduction

Conclusions

References

Tables

Figures



Back

Close

Full Screen / Esc

Printer-friendly Version

Interactive Discussion



**Tropospheric NO₂
columns over East
Asia**

K. M. Han et al.

[Title Page](#)[Abstract](#)[Introduction](#)[Conclusions](#)[References](#)[Tables](#)[Figures](#)[◀](#)[▶](#)[◀](#)[▶](#)[Back](#)[Close](#)[Full Screen / Esc](#)[Printer-friendly Version](#)[Interactive Discussion](#)

Table 1 summarizes base-case simulation and several sensitivity runs for this study. For the base-case simulation, monthly variations of the anthropogenic NO_x emissions from Zhang et al. (2009) were considered for China, while those from Han et al. (2009) were used for South Korea and Japan. As shown in Fig. 1, the monthly variations in NO_x emissions over China were highly uncertain. This uncertainty is explored and discussed in Sect. 3.2.1.

The modeling period was from 1 January to 31 December 2006. In this study, 2006 was chosen for the CMAQ model simulations, because relatively accurate emission data of INTEX-B over China are available for this year. The horizontal domain covers from 100° E to 150° E and from 20° N to 50° N with a grid-resolution of 30 km × 30 km. The vertical domain covers from 1000 hPa to 118 hPa with 14 terrain following σ-coordinates. For considering aerosol dynamics and thermodynamics, the aerosol module of AERO4 was selected (Binkowski and Roselle, 2003).

For the consideration of gas-phase chemistry, the SAPRAC-99 (Statewide Air Pollution Research Center-99) mechanism was selected (Carter, 2000). Then, to consider unknown OH radical processes (Lelieveld et al., 2008), the SAPRAC-99 mechanism was modified partly, based on the work of Butler et al. (2008) in the following way (Reaction R1):



Here, ISOPO₂ and ISOPOOH represent isoprene-derived peroxy radical and peroxide, respectively. Other schemes used in the CMAQ model simulations were the global mass-conserving scheme (YAMO) for horizontal and vertical advection (Yamartino, 1993), the asymmetric convective model (ACM) algorithm for convective cloud mixing, and ACM (ver. 2) for vertical diffusion (Pleim, 2007).

In the CMAQ modeling, initial conditions (ICs) were prepared from 1 week-long spin-up model simulations, and boundary conditions (BCs) were obtained from global CTM simulations, MOZART (Model for OZone And Related chemical Tracers) (Emmons et al., 2010). The MOZART model simulation data for the BCs were obtained

from <http://www.acd.ucar.edu/wrf-chem/mozart.shtml>. Other details about the modeling conditions were reported by Han et al. (2013).

For synchronization with the OMI-observed tropospheric Ω_{NO_2} , CMAQ-estimated tropospheric Ω_{NO_2} data were collected and then averaged between 13:00 and 14:00 local time (LT), because the OMI sensor scans the atmosphere over East Asia approximately at 13:45 LT. For further detailed analyses, eight highly-populated focus regions were defined in this study, and are presented in Fig. 2.

2.2 OMI-retrieved NO_2 columns and AKs

The OMI instrument on board the NASA/EOS–Aura satellite, a nadir-viewing imaging spectrometer, provides information on the properties of aerosols and clouds as well as global levels of atmospheric species such as ozone, NO_2 , SO_2 , OCIO, BrO, and HCHO on a daily basis via observing backscattered UV-VIS radiances from 270 to 550 nm (Levelt et al., 2006). Two-dimensional charge-coupled device (CCD) detectors equipped in the OMI instrument observe the atmosphere with a spatial resolution of $13\text{ km} \times 24\text{ km}$. CCD1 covers the UV channel of 270–310 nm and 310–365 nm. The visible channel, ranging from 365 to 500 nm, is covered by CCD2 to observe NO_2 .

In this study, daily levels of OMI-retrieved tropospheric NO_2 columns from KNMI/DOMINO v2.0 products were used (Boersma et al., 2007, 2011). The KNMI/DOMINO v2.0 algorithm (hereafter, KNMI algorithm) for retrieving the tropospheric NO_2 columns from the OMI radiance data proceeds in the following sequence. First, a slant NO_2 column density was determined from spectral fitting, using the differential optical absorption spectroscopy (DOAS) method. Second, the stratospheric NO_2 contribution was removed by subtracting the stratospheric portions of slant NO_2 columns calculated from the global CTM, TM4, from the total slant NO_2 columns. Finally, the tropospheric slant NO_2 columns were converted into vertical NO_2 columns, using the air mass factor (AMF), defined as the ratio of the measured slant column to the vertical column. This AMF is a function of several factors, such as the satellite

Tropospheric NO_2 columns over East Asia

K. M. Han et al.

[Title Page](#)[Abstract](#)[Introduction](#)[Conclusions](#)[References](#)[Tables](#)[Figures](#)[Back](#)[Close](#)[Full Screen / Esc](#)[Printer-friendly Version](#)[Interactive Discussion](#)

viewing geometry, surface albedo, surface pressure, and vertical distributions of clouds, aerosols, and trace gases.

In this study, to reduce retrieval errors, measured scenes with surface albedo values larger than 0.3 were excluded, as suggested by Boersma et al. (2011). Also, observed pixels with cloud radiance fractions (CRF) larger than 50 % were filtered out, which are approximately equivalent to cloud fractions (CF) smaller than 20 % (van der A et al., 2006). Thus, OMI-retrieved tropospheric NO₂ columns under almost “cloud-free” conditions were used in this study.

The AKs were also applied to the CMAQ model simulations. The AKs are analytically expressed in Eq. (1) (Rodgers, 2000; Eskes and Boersma, 2003):

$$\begin{aligned} AK &= G_y K_x \\ &= \frac{\partial R}{\partial y} \frac{\partial F}{\partial x} \\ &= \frac{\partial \hat{x}}{\partial x} \end{aligned} \quad (1)$$

where G_y and K_x represent the sensitivities of the retrieval (R) to the measurement (y) and the forward model (F) to the state (x), respectively. Also, K_x is known as a weighting function or Jacobian matrix. Thus, as shown in Eq. (1), the AKs represent the sensitivity of the retrieved quantities (here, vertical NO₂ column, \hat{x}) to the true atmospheric state (x). Using the AKs, the retrieved quantity (\hat{x}) can be expressed by Eq. (2):

$$\hat{x} - x_a = AK(x - x_a) + \varepsilon \quad (2)$$

where x_a and ε represent a prior estimate and total error in measured signal relative to the forward model, respectively. Information on the AKs and retrieved quantity are included in the daily KNMI products (http://www.temis.nl/airpollution/no2col/no2regioomi_v2.php).

Figure 3 presents the vertical distributions of the seasonally-averaged AKs retrieved from the KNMI algorithms over Central East China (CEC) and other regions (defined in

Tropospheric NO₂ columns over East Asia

K. M. Han et al.

Title Page

Abstract Introduction

Conclusions References

Tables Figures

◀ ▶

◀ ▶

Back Close

Full Screen / Esc

Printer-friendly Version

Interactive Discussion



Tropospheric NO₂ columns over East Asia

K. M. Han et al.

Title Page

Abstract

Introduction

Conclusions

References

Tables

Figures



Back

Close

Full Screen / Esc

Printer-friendly Version

Interactive Discussion



Fig. 2). As shown in Fig. 3, the AKs are strongly altitude-dependent in the troposphere. For example, near the surface, the AKs are smaller than unity, indicating that the OMI observations are under-sensitive, by the extent deviated from the vertical line of unity. In contrast, in the upper troposphere, the AKs are larger than unity, indicating that the OMI measurements are over-sensitive, by the extent deviated from the line of unity (an AK of unity means that the OMI instruments can directly measure the true NO₂ column densities). Additionally, the AKs are generally lower in warm seasons than in cold seasons. These lower values in the AKs during the summer are probably related to the lower surface albedos and the lower concentrations of aerosols during the summer (Eskes and Boersma, 2003).

Once the CMAQ model simulations were done, the AKs were applied under the almost cloud-free conditions. The tropospheric Ω_{NO_2} values were also retrieved from the OMI observations via the KNMI algorithms. Then, using the two NO₂ columns, a comparison study was made between the two Ω_{NO_2} products. Figure 4 illustrates the main processes of the comparison study.

3 Results and discussions

The objective of this study was to examine the accuracy of the NO_x emission fluxes over East Asia by comparing two tropospheric Ω_{NO_2} obtained from the CMAQ model simulations and OMI observations (Sect. 3.1). Several sensitivity analyses were also conducted to examine the influences of the uncertainty factors that can result in discrepancies between $\Omega_{\text{NO}_2, \text{CMAQ}}$ and $\Omega_{\text{NO}_2, \text{OMI}}$ (Sect. 3.2). Obviously, not all the influential factors can be explored within the framework of this study. Thus, several selected issues that may be important are also discussed further in Sect. 3.2.4.

3.1 Comparison between CMAQ-estimated and OMI-retrieved NO₂ columns: Case 1

3.1.1 $\Omega_{\text{NO}_2, \text{CMAQ}}$ vs. $\Omega_{\text{NO}_2, \text{OMI}}$

In this study, the analyses were conducted for four seasons: (i) Spring (March–May 2006), (ii) Summer (June–August 2006), (iii) Fall (September–November 2006), and (iv) Winter (December–February 2006). For more detailed analyses, eight focus regions were also defined: (i) Central East China (CEC), (ii) Central East China 2 (CEC2), (iii) South China (SC), (iv) Sichuan Basin (SB), (v) South Korea (SK), (vi) the western part of Japan (JP1), (vii) the eastern part of Japan (JP2), and (viii) the entire domain (DM) (refer to Fig. 2 regarding the domains).

Figure 5 presents the comparison analysis between the $\Omega_{\text{NO}_2, \text{CMAQ}}$ and $\Omega_{\text{NO}_2, \text{OMI}}$ for the four seasons over East Asia before and after the applications of the AKs. As shown in Fig. 5, the CMAQ model simulations (the first and second columns) show spatially and seasonally consistent patterns with OMI observations (the third column). For example, the high values of the $\Omega_{\text{NO}_2, \text{OMI}}$ over the densely populated and economically developed mega-city regions such as Beijing, Shanghai, Hong Kong, Seoul, and Tokyo (refer to Fig. 2 regarding their locations) are well captured by the CMAQ model simulations. Also, the low values of the Ω_{NO_2} from the CMAQ model simulation during the summer are well matched with those from the OMI observations. The lower levels of the Ω_{NO_2} during the summer are possibly caused by active NO_x chemical losses via the reaction of NO₂ with OH radicals (Han et al., 2009). Because of this “fast chemical NO_x loss rate” during the summer, summer is not the season of primary interest in this study, because there are many uncertainties and unknowns related to these chemical NO_x loss rates and processes in the CTMs (Han et al., 2009). These uncertainties and unknown factors will be discussed further in Sect. 3.2.4. In the same context, more attention was paid to winter (spring and fall) in this study, because there are fewer uncertainties and unknowns related to the chemical NO_x loss rates during these seasons. Additionally, the levels of the Ω_{NO_2} during the winter are distinctly high.

These high values would be better for a comparison study between the $\Omega_{\text{NO}_2, \text{CMAQ}}$ and $\Omega_{\text{NO}_2, \text{OMI}}$, as shown in Fig. 5.

When panels a and c in Fig. 5 are compared, it can be seen that the $\Omega_{\text{NO}_2, \text{CMAQ}}$ is in general greatly larger than the $\Omega_{\text{NO}_2, \text{OMI}}$ over the entire domain. The large differences between the two NO_2 columns can be confirmed again in panel a of Fig. 6. Previously, Han et al. (2009, 2011) also compared the CMAQ-calculated NO_2 columns with satellite-retrieved NO_2 columns, without using the AKs, to investigate the accuracy of bottom-up NO_x emissions over East Asia. Based on this comparison, Han et al. (2011) concluded that the bottom-up NO_x emissions used in the CTM simulation over East Asia could be overestimated. However, such a comparison without applying the AKs is like comparing apples and oranges, and is not reasonable. Such studies have been conducted over East Asia, with misleading conclusions (e.g. Ma et al., 2006; He et al., 2007; Uno et al., 2007; Shi et al., 2008; Han et al., 2009, 2011). In this context, we now wish to correct our previous conclusions (Han et al., 2011) here, applying the AKs to the CMAQ model simulations, using the linear relationship presented in Eq. (2).

After the application of the AKs to the CMAQ model simulations, the comparison becomes independent of a prior profile shape used in the retrieval (Eskes and Boersma, 2003). In this study, when the panels b and c in Fig. 5 are compared, it can be seen that the CMAQ-calculated NO_2 columns considering the AKs are much more comparable to the OMI-retrieved NO_2 columns, possibly indicating that the bottom-up NO_x emission used in the CMAQ model simulations would not be very greatly overestimated, unlike the previous conclusion in Han et al. (2011). Figure 6 more directly shows the effects of the application of the AKs. When the AKs are applied, the differences are greatly diminished, and are even negative, particularly over the CEC regions. The $\Omega_{\text{NO}_2, \text{CMAQ}, \text{AK}}$ becomes smaller than the $\Omega_{\text{NO}_2, \text{OMI}}$ over the CEC, SC, SK, JP1, and JP2 regions. Also, possible overestimations of the bottom-up NO_x emissions were found in the CEC2 and SB regions, particularly during the winter. In Table 2, we summarize the average tropospheric NO_2 columns and normalized mean errors (NMEs) with and without considering the AKs for the eight focus regions. After the applications of the AKs, it can

Tropospheric NO_2
columns over East
Asia

K. M. Han et al.

Title Page

Abstract

Introduction

Conclusions

References

Tables

Figures



Back

Close

Full Screen / Esc

Printer-friendly Version

Interactive Discussion



be seen that the NMEs are greatly reduced during all seasons, except for the summer, over the entire domain (from $\sim 103\%$ to $\sim 46\%$, from $\sim 112\%$ to $\sim 45\%$, and from $\sim 135\%$ to $\sim 40\%$, during spring, fall, and winter, respectively).

Collectively, we found that the application of the AKs is an essential component for a direct comparison between model- and satellite-derived NO_2 columns. It was found that after the applications of the AKs, the differences between the two NO_2 columns were greatly reduced. To further investigate the eight regions of interest, scatter plots and statistical analyses were carried out in Sect. 3.1.2.

3.1.2 Scatter plots and statistical analyses

Figure 7 presents the seasonal scatter plot analysis between the $\Omega_{\text{NO}_2, \text{CMAQ}, \text{AK}}$ and $\Omega_{\text{NO}_2, \text{OMI}}$ for the seven focus regions defined in Fig. 2. The statistical analysis related to the scatter plots was also conducted in terms of the Pearson correlation coefficient (R) and linear regression slope (S). Although the correlation coefficients were sometimes lower than 0.7 in Fig. 7, the two NO_2 columns correlated well, with R values between 0.71 and 0.94 (also, refer to the “ R ” values colored in Fig. 8). Slopes lower than 1.0 (see dashed lines in Fig. 7) were also found in the “blue” regions in Fig. 6 such as the CEC, SC, SB, JP1, and JP2 regions. These low slopes indicate the possible “underestimation” of the bottom-up NO_x emissions used in the CMAQ model simulations, as discussed in Sect. 3.1.1.

Further statistical analyses were conducted. For absolute differences, Mean Error (ME) and Mean Bias (MB) were utilized. For relative differences, Mean Normalized Gross Error (MNGE), Mean Normalized Bias (MNB), Normalized Mean Error (NME), Normalized Mean Bias (NMB), Mean Fractional Error (MFE), and Mean Fractional Bias (MFB) were used. The Pearson correlation coefficient (R) and index of agreement (IOA) were also analyzed to assess the degrees of correlations and agreement, respectively. These 10 performance metrics are defined in Table A1 (see Appendix A). As shown in Fig. 8, the IOAs (as a measure of the degree of model prediction errors, Willmott, 1981) showed high values, between 0.78 and 0.93, over the entire domain. However, the

Title Page

Abstract

Introduction

Conclusions

References

Tables

Figures



Back

Close

Full Screen / Esc

Printer-friendly Version

Interactive Discussion



Tropospheric NO₂ columns over East Asia

K. M. Han et al.

Title Page

Abstract

Introduction

Conclusions

References

Tables

Figures



Back

Close

Full Screen / Esc

Printer-friendly Version

Interactive Discussion



study still has several uncertainties. Among them, first, the monthly variations of NO_x emissions over China were investigated, using different monthly variations as shown in Fig. 1. In this sensitivity run, we applied a more drastic monthly variation of the NO_x emissions in China (thick-black line in Fig. 1) (Han et al., 2009). The main reason we did this is that, as shown in Figs. 5–7, the $\Omega_{\text{NO}_2, \text{CMAQ, AK}}$ was underestimated, compared with the $\Omega_{\text{NO}_2, \text{OMI}}$, over several regions (such as CEC and main mega-city areas like Hong Kong and Shanghai) in China, particularly during the cold months.

The results are presented in Fig. 9. The spatial distributions of the $\Omega_{\text{NO}_2, \text{CMAQ, AK}}$ and $\Omega_{\text{NO}_2, \text{OMI}}$ are shown in Fig. 9 for the four seasons. As indicated in Supplement Table S1 in the supplementary materials, the application of the AKs again greatly reduced the errors and biases between the two tropospheric NO₂ columns in this sensitivity test. As expected, the $\Omega_{\text{NO}_2, \text{CMAQ, AK}}$ in Fig. 9a generally increased for the spring and winter, whereas it decreased for the summer and fall, compared with the values in Fig. 5b. These increases in the $\Omega_{\text{NO}_2, \text{CMAQ, AK}}$ for the winter produced better agreement with the $\Omega_{\text{NO}_2, \text{OMI}}$, particularly over the CEC region (see the average NO₂ columns and NMEs in Tables 2 and Supplement Table S1). However, as shown in Tables 2 and Supplement Table S1, the situations became worse, except for the CEC region, showing significant increases in NMEs, compared with the NMEs in cases using of the monthly variation of the INTEX-B inventory. Even larger (more serious) differences between the two NO₂ columns in Fig. 9c were found over other regions of China (CEC2, SC, and SB) than those shown in Fig. 6b in terms of errors and biases. Collectively, it appears that the monthly variations of the OMI observations are better captured by the CMAQ model simulations using the monthly variations of the INTEX-B inventory than those from Han et al. (2009). Further detailed analyses over the eight focus regions were carried out, and the scatter plots and statistical analyses are presented in Supplement Figs. S1 and S2 of the supplementary materials. Although it can be concluded that the monthly variation of the INTEX-B NO_x inventory appears to be more realistic, the monthly variations in the NO_x emissions in China are important, though still uncertain. Accurate information on this important issue should be examined in future comparison studies.

3.2.2 Another NO_x emission inventory (REAS): Case 3

There is another NO_x emission inventory available in China: the REAS emission inventory. Thus, in this section, the REAS emission inventory, a frequently used bottom-up inventory established by the National Institute of Environmental Studies (NIES) in Japan, was tested over China for January (a cold month). Because the REAS inventory does not include monthly variation, the same monthly variation of the INTEX-B inventory was also applied to this sensitivity study. The strength of the NO_x emissions between the INTEX-B and REAS inventories differed greatly over China. For example, the total annual NO_x emissions from the INTEX-B inventory were 5.41, 4.85, 3.49, and 1.24 Tg yr⁻¹ over the CEC, CEC2, SC, and SB regions, respectively, whereas those from the REAS inventory were 4.21, 3.40, 3.04, and 0.88 Tg yr⁻¹, respectively, over the same regions.

The results are presented in Fig. 10 and Supplement Table S2. The application of the AKs to the CMAQ model simulations were also taken into account in this comparison (see Table S2 in the Supplement). As expected, the $\Omega_{\text{NO}_2, \text{CMAQ, AK}}$ decreased significantly over China, when the REAS NO_x emissions are used (refer to Table S2 in the Supplement). Although the absolute differences between the $\Omega_{\text{NO}_2, \text{CMAQ, AK}}$ and $\Omega_{\text{NO}_2, \text{OMI}}$ became smaller over the CEC2 and SB regions, much large underestimates were found over the CEC region, compared with the case of the INTEX-B inventory as shown in Fig. 10. Recently, Kurokawa et al. (2013) reported that the NO_x emissions from the REAS inventory were possibly underestimated, by a factor of ~ 0.9, over China for the year of 2006.

Collectively, our results indicate that (i) the NO_x emission fluxes from the REAS inventory were also underestimated over China (particularly, over the CEC region), (ii) both NO_x emission inventories (INTEX-B and REAS) show underestimation over the CEC region and the Hong Kong area, and (iii) accurate spatial distributions of NO_x emissions and the strength of NO_x emissions are important factors to reduce the degree of disagreement between the CTM-estimated and satellite-retrieved NO₂

Tropospheric NO₂ columns over East Asia

K. M. Han et al.

Title Page

Abstract

Introduction

Conclusions

References

Tables

Figures



Back

Close

Full Screen / Esc

Printer-friendly Version

Interactive Discussion



Tropospheric NO₂ columns over East Asia

K. M. Han et al.

Title Page

Abstract

Introduction

Conclusions

References

Tables

Figures



Back

Close

Full Screen / Esc

Printer-friendly Version

Interactive Discussion



columns. For better agreement between the $\Omega_{\text{NO}_2, \text{CMAQ, AK}}$ and $\Omega_{\text{NO}_2, \text{OMI}}$ over China, a combination of the two emission inventories may be a good practical attempt in the CMAQ model simulations over East Asia, based on this result. That is, the INTEX-B NO_x emissions data tended to produce better results over the CEC region, whereas the REAS NO_x emissions data tended to generate better results over the CEC2 and SB regions. However, this issue needs a more sophisticated approach and should be investigated further.

3.2.3 Reaction probability of N₂O₅: Case 4

We explored the issue of reaction probability of N₂O₅ ($\gamma_{\text{N}_2\text{O}_5}$) onto aerosols, because a relatively large discrepancy between the $\Omega_{\text{NO}_2, \text{CMAQ, AK}}$ and $\Omega_{\text{NO}_2, \text{OMI}}$ was found, particularly during the winter season. As mentioned previously, we paid more attention to the cold seasons, such as winter, fall, and spring, because the cold months are better for conducting this type of study due to the uncertain tropospheric chemistry and faster NO_x loss rates during the summer.

In particular, during the winter season, the condensation of N₂O₅ into atmospheric particles is an important NO_x loss process (Dentener and Crutzen, 1993; Brown et al., 2004, 2006). Thus, it can affect the CMAQ-simulated NO₂ columns ($\Omega_{\text{NO}_2, \text{CMAQ, AK}}$). Although it is an important physico-chemical NO_x loss process during the winter, the magnitude of $\gamma_{\text{N}_2\text{O}_5}$ has been a controversial issue. In this study, five $\Omega_{\text{NO}_2, \text{CMAQ, AK}}$ from the CMAQ model simulations with five different $\gamma_{\text{N}_2\text{O}_5}$ parameterizations were compared with the $\Omega_{\text{NO}_2, \text{OMI}}$ over East Asia. These five parameterizations are from the works of: (i) Dentener and Crutzen (1993), (ii) Riemer et al. (2003), (iii) a combination of Riemer et al. (2003) and Evans and Jacob (2005), (iv) Davis et al. (2008), and (v) Brown et al. (2006). The mathematical expressions for these parameterizations are summarized briefly in Table 3. In the Dentener and Crutzen's parameterization (1993), they used a fixed value of $\gamma_{\text{N}_2\text{O}_5}$ of 0.1 in their global CTM simulation (Scheme I in Table 3). In Riemer et al.'s parameterization (2003), $\gamma_{\text{N}_2\text{O}_5}$ is a main function of the acidity of the particles (Scheme II). In the combined parameterization of Evan and Jacob (2006) and

Tropospheric NO₂ columns over East Asia

K. M. Han et al.

Title Page

Abstract

Introduction

Conclusions

References

Tables

Figures



Back

Close

Full Screen / Esc

Printer-friendly Version

Interactive Discussion



Rierner et al. (2003), $\gamma_{\text{N}_2\text{O}_5}$ is a function of relative humidity (RH), temperature, and the acidity of the particles (Scheme III, standard scheme). In Davis et al. (2008)'s parameterization, $\gamma_{\text{N}_2\text{O}_5}$ is a function of all the factors, such as RH, temperature, the acidity of the particles, and the mixing state (Scheme IV). Finally, for Brown et al. (2006)'s parameterization, we used a fixed minimum value of $\gamma_{\text{N}_2\text{O}_5}$ of 10^{-3} in the CMAQ model simulation (Scheme V).

The comparison results are presented in Fig. 11. As shown in Fig. 11 and Table 4, the $\Omega_{\text{NO}_2, \text{CMAQ, AK}}$ with the Brown et al. (2006) parameterization were 19 % larger than those with the standard Scheme (III) over East Asia. This indicates that Brown et al.'s parameterization resulted in the smallest NO_x loss rates (or nitrate formation rates) via this physico-chemical reaction pathway. In contrast, the application of the Dentener and Crutzen's parameterization to the CMAQ model simulation produced the smallest $\Omega_{\text{NO}_2, \text{CMAQ, AK}}$ in East Asia, indicating the fastest NO_x loss rates, due to the large $\gamma_{\text{N}_2\text{O}_5}$. These results suggest that Brown et al.'s $\gamma_{\text{N}_2\text{O}_5}$ (0.001) may be smaller than the real value, while Dentener and Crutzen's $\gamma_{\text{N}_2\text{O}_5}$ (0.1) is probably larger. Other than Brown et al.'s and Dentener and Crutzen's parameterizations, it was found that there was almost no significant or practical difference in the $\Omega_{\text{NO}_2, \text{CMAQ, AK}}$ among the other three Schemes, II, III, and IV (also, refer to Table 4).

As shown in Fig. 11 and Table 4, Schemes II, III, and IV tended to produce better $\Omega_{\text{NO}_2, \text{CMAQ, AK}}$ data over East Asia than Schemes I and V, compared with $\Omega_{\text{NO}_2, \text{OMI}}$. More recently, Brown et al. (2009) and Bertram et al. (2009) also discussed that the $\gamma_{\text{N}_2\text{O}_5}$ values being used currently in regional/global CTMs were generally larger than those from their observed $\gamma_{\text{N}_2\text{O}_5}$. In addition to the issue of $\gamma_{\text{N}_2\text{O}_5}$, it should be noted that the aerosol surface density (A) is another uncertain factor that can influence the $\Omega_{\text{NO}_2, \text{CMAQ, AK}}$, because the rate constant ($k_{\text{N}_2\text{O}_5}$) of the physico-chemical reaction also depends on the aerosol surface density (refer to the Schwartz formula, $k_{\text{N}_2\text{O}_5} = \frac{A \times C_{\text{mean}} \gamma_{\text{N}_2\text{O}_5}}{4}$). Although all of these issues are arguable, our results show that the $\gamma_{\text{N}_2\text{O}_5}$ parameterizations can certainly influence the levels of Ω_{NO_2} in East Asia, particularly during the winter season.

3.2.4 More uncertainties and outlooks

As mentioned previously, in this type of analysis all types of temporal variation are potentially important and should therefore be taken into account. A sensitivity analysis on the monthly variation in the NO_x emissions in China was performed in Sect. 3.2.1, showing that the monthly variations in NO_x emissions were an important factor. In contrast, there is only limited information on other temporal variation, such as daily and weekly variation in NO_x emissions in East Asia. Unfortunately, no emission inventory in East Asia can provide us with this level of information. Although not shown here, we did also test daily variation in NO_x emissions, based on hourly NO₂ concentrations measured in the megacities. However, it has been found that there is no significant impact of this daily variation on the $\Omega_{\text{NO}_2, \text{CMAQ}, \text{AK}}$ at 13:00 LT (the OMI local pass time). However, this issue should be investigated further. Regarding the issue of the temporal variation, it can be suggested that the future Korean Geostationary Environmental Monitoring Spectrometer (GEMS) sensor, which is planned to be launched in 2018, will/may be able to help to obtain such information on daily and weekly variation in the NO_x emissions over East Asia (Kim, 2012).

There is also some level of uncertainty in the NO₂-to-NO ratios, as discussed previously by Richter et al. (2005) and Han et al. (2009). This factor may be important, because every satellite remote-sensor monitors only NO₂ columns, not NO_x columns. The NO₂-to-NO ratios are affected seriously by anthropogenic and biogenic VOC (AVOC and BVOC) emissions and their mixing ratios. For example, if we assume a photo-stationary state, the NO₂-to-NO ratios can be influenced by the mixing ratios of ozone and HO₂, CH₃O₂, and RO₂ radicals, as shown in the following formula:

$$\frac{[\text{NO}_2]}{[\text{NO}]} = \frac{k_1[\text{O}_3] + k_2[\text{HO}_2] + k_3[\text{CH}_3\text{O}_2] + k_4[\text{RO}_2]}{J_1} \quad (3)$$

where J_1 is the NO₂ photolysis rate constant (s⁻¹) and k_1 , k_2 , k_3 , and k_4 are the reaction constants (cm³ molecules⁻¹ s⁻¹) for NO + O₃, NO + HO₂, NO + CH₃O₂, and

Title Page

Abstract

Introduction

Conclusions

References

Tables

Figures



Back

Close

Full Screen / Esc

Printer-friendly Version

Interactive Discussion



NO+RO₂ reactions, respectively. The mixing ratios of ozone, HO₂, CH₃O₂, and RO₂ in Eq. (3) can be affected by AVOC and BVOC emissions and their mixing ratios, which are believed to be highly uncertain in East Asia (Fu et al., 2007; Lin et al., 2012; Han et al., 2013).

5 Third, as also discussed by Han et al. (2009), there is large uncertainty in the NO_x loss rates in global/regional CTMs. Many groups have reported that the uncertainty in the NO_x loss rate is related to several factors (Lin et al., 2012; Stavrou et al., 2013), such as nitric acid formation (Atkinson et al., 2004; Butkovskaya et al., 2005, 2009; Mollner et al., 2010; Sander et al., 2011; Henderson et al., 2012), isoprene chemistry
10 (e.g. OH regeneration) during the summer months (Butler et al., 2008; Lelieveld et al., 2008; Archibald et al., 2010; Kubistin et al., 2010; Pugh et al., 2010), alkyl nitrate formation (Browne and Cohen, 2012; Browne et al., 2013), and “daytime” HONO chemistry (Harris et al., 1982; Svennson et al., 1987; Rondon and Sanhueza, 1989; Pagsberg et al., 1997; Stemmler et al., 2006; Sörgel et al., 2011; Zhou et al., 2011). All of these
15 issues are on-going and open questions. These uncertainties in the NO_x loss rates can obviously affect the conclusions of this type of study to some degree.

In addition to the issues mentioned above, in the CTM simulations there are additional uncertainties in geogenic NO_x emissions (e.g., soil NO_x emissions) and pyrogenic NO_x emissions (e.g., biomass burning NO_x emissions) (Bertram et al., 2005; Jaeglé et al., 2005; Hudman et al., 2010; Lin, 2012). However, for example, geogenic
20 NO_x emissions are usually more active during the summer. During the summer, the NO_x loss rates are so fast that considerations of additional geogenic NO_x emissions would hardly change the CTM-calculated NO₂ columns (Boersma et al., 2009; Han et al., 2009). The same is true for the issues of OH recycling and isoprene-derived
25 alkyl nitrate formation mentioned above. There are uncertainties and unknown chemistry related to isoprene, but, again, due to the fast NO_x loss rates during the summer, it has been found that these factors do not greatly affect the $\Omega_{\text{NO}_2, \text{CMAQ}, \text{AK}}$ during the summer in our test runs (data not shown). This is why we said that the summer was not a season of major interest in this study.

Tropospheric NO₂ columns over East Asia

K. M. Han et al.

Title Page

Abstract

Introduction

Conclusions

References

Tables

Figures



Back

Close

Full Screen / Esc

Printer-friendly Version

Interactive Discussion



Tropospheric NO₂ columns over East Asia

K. M. Han et al.

Title Page

Abstract

Introduction

Conclusions

References

Tables

Figures



Back

Close

Full Screen / Esc

Printer-friendly Version

Interactive Discussion



On the other hand, in the view of satellite observations, there are errors and uncertainties in the retrievals of the NO₂ vertical columns and the AKs. There are also several NO₂ vertical column products from different sensors (e.g. GOME, OMI, SCIAMACHY, and GOME-2) and from different algorithms (e.g. KNMI, Bremen, BIRA, and NASA). For example, the different NO₂ products sometimes show considerable differences (Herron-Thorpe et al., 2010). Also, Boersma et al. (2011) reported that the tropospheric NO₂ columns retrieved from the DOMINO v2.0 algorithm showed 20 % and 10 % lower values in the winter and summer, respectively, over polluted areas, such as the CEC region in China, compared with values from DOMINO v1.02. Overall, different combinations of these sensors and algorithms can produce different NO₂ column products. Thus, in this type of comparison analysis, all the uncertainty factors mentioned should be taken into account cautiously.

4 Summary and conclusions

The accuracy of bottom-up NO_x emission fluxes from the INTEX-B, CAPSS, and REAS emission inventories were investigated through comparisons between the $\Omega_{\text{NO}_2, \text{CMAQ, AK}}$ and $\Omega_{\text{NO}_2, \text{OMI}}$ in East Asia. For the comparison study, the CMAQ model simulations were carried out over 12 months in 2006 over East Asia. Also, for the direct comparison between the $\Omega_{\text{NO}_2, \text{CMAQ}}$ and $\Omega_{\text{NO}_2, \text{OMI}}$, we applied the AKs to the CMAQ model simulations.

It was found that after the applications of the AKs, the CMAQ-estimated NO₂ columns were much more comparable to the OMI-retrieved NO₂ columns over East Asia and that the normalized mean errors (NMEs), for example, decreased, from ~ 103 % to ~ 46 %, from ~ 112 % to ~ 45 %, and from ~ 135 % to ~ 40 % in East Asia during the spring, fall, and winter, respectively. Overall, the bottom-up NO_x emissions were, on annual average, ~ 28 % (with seasonal variation of ~ 7 to ~ 60 %) underestimated in East Asia, although some overestimates were also found partly over the CEC2, SB, and SK regions during the winter.

Tropospheric NO₂ columns over East Asia

K. M. Han et al.

Title Page

Abstract

Introduction

Conclusions

References

Tables

Figures



Back

Close

Full Screen / Esc

Printer-friendly Version

Interactive Discussion



To assess the seasonal and spatial discrepancies, several sensitivity studies, shown in Table 1, were performed considering several uncertainty factors such as (i) monthly variation of NO_x emission, (ii) strength of NO_x emission, and (iii) reaction probabilities of N₂O₅. In Table 5, we summarize the relative changes in the NO₂ columns from the sensitivity simulations with respect to those from the standard simulation (Case 1). From the sensitivity simulations, we found that:

- monthly variations in NO_x emissions have a strong impact on tropospheric NO₂ columns. The relative changes ranged from −31.15 % to 66.03 % over China, when the monthly factors from Han et al. (2009) were used. However, Han et al.'s monthly variations (2009) resulted in even larger discrepancies between $\Omega_{\text{NO}_2, \text{CMAQ, AK}}$ and $\Omega_{\text{NO}_2, \text{OMI}}$ over several regions in China.
- As shown in Table 5, when REAS inventory data over China were used in the CMAQ model simulations, the $\Omega_{\text{NO}_2, \text{CMAQ, AK}}$ were lower by −31.50 % to −58.33 % over China than those from the case with the INTEX-B inventory. Based on this, the NO_x emissions from the REAS NO_x emissions appeared to be more underestimated over China than the INTEX-B NO_x emissions.
- In the sensitivity test of $\gamma_{\text{N}_2\text{O}_5}$, almost no difference in the $\Omega_{\text{NO}_2, \text{CMAQ, AK}}$ was found among the conventional $\gamma_{\text{N}_2\text{O}_5}$ parameterizations. However, the $\Omega_{\text{NO}_2, \text{CMAQ, AK}}$ from Brown et al. (2006)'s parameterization were 18.25 % larger over East Asia than the $\Omega_{\text{NO}_2, \text{CMAQ, AK}}$ from the combined parameterization of Riemer et al. (2003) and Evans and Jacob (2006). Thus, it appeared that the $\gamma_{\text{N}_2\text{O}_5}$ parameterization would not be a negligible factor, particularly during the winter.

Although we have listed several uncertainty factors in this study, we believe that the application of the AKs was the single most dominant factor that can affect the $\Omega_{\text{NO}_2, \text{CMAQ, AK}}$. Additionally, the strength and monthly variation in NO_x emissions can also significantly influence the levels of tropospheric $\Omega_{\text{NO}_2, \text{CMAQ, AK}}$ in East Asia. Moreover, we showed that the $\gamma_{\text{N}_2\text{O}_5}$ parameterization could be another important factor

in the winter. Because other possible uncertainty factors still exist, as discussed in Sect. 3.2.4, further analyses are necessary in future studies.

The estimation of “top-down” NO_x emissions has also been carried out in East Asia (Stavrakou et al., 2008; Lin et al., 2010; Mijling et al., 2013) using satellite-derived NO_2 columns. However, in such top-down estimations, there are other uncertain (limiting) factors, such as lifetimes of NO_x (i.e., τ_{NO_x}). The uncertainty is also linked with the factors we discussed in Sect. 3.2.4. Improvements in the NO_x emissions data or the evaluation of the accuracy of the bottom-up NO_x emission fluxes in East Asia can improve air quality modeling and chemical weather forecast over East Asia. Thus, much efforts should be focused on this issue in future, particularly over East Asia. In the same context, many efforts on inverse modeling to improve the accuracy of NO_x emissions data over East Asia such as adjoint modeling with measured data and top-down estimations of the NO_x emissions with satellite observations could also contribute to improving the performance of air quality modeling and the accuracy of chemical weather forecasting over East Asia (Park et al., 2013).

The Supplement related to this article is available online at [doi:10.5194/acpd-14-17585-2014-supplement](https://doi.org/10.5194/acpd-14-17585-2014-supplement).

Acknowledgements. This research was supported by the GEMS program of the Ministry of Environment, Korea and the Eco Innovation Program of KEITI (2012000160004). This work was also funded by the Eco-Innovation project 411-113-013 from Korean Ministry of Environment and partly supported by the Korea Meteorological Administration Research and Development Program under Grant CATER 2012-7110. We acknowledge the use of the tropospheric NO_2 column data from www.temis.nl.

**Tropospheric NO_2
columns over East
Asia**

K. M. Han et al.

Title Page

Abstract

Introduction

Conclusions

References

Tables

Figures



Back

Close

Full Screen / Esc

Printer-friendly Version

Interactive Discussion



Appendix A

For statistical analyses between the CMAQ-calculated and OMI-retrieved NO₂ columns, several statistical parameters below are introduced in Table A1.

References

- 5 Archibald, A. T., Cooke, M. C., Utembe, S. R., Shallcross, D. E., Derwent, R. G., and Jenkin, M. E.: Impacts of mechanistic changes on HO_x formation and recycling in the oxidation of isoprene, *Atmos. Chem. Phys.*, 10, 8097–8118, doi:10.5194/acp-10-8097-2010, 2010.
- 10 Atkinson, R., Baulch, D. L., Cox, R. A., Crowley, J. N., Hampson, R. F., Hynes, R. G., Jenkin, M. E., Rossi, M. J., and Troe, J.: Evaluated kinetic and photochemical data for atmospheric chemistry: Volume I – gas phase reactions of O_x, HO_x, NO_x and SO_x species, *Atmos. Chem. Phys.*, 4, 1461–1738, doi:10.5194/acp-4-1461-2004, 2004.
- Bertram, T. H., Heckel, A., Richter, A., Burrows, J. P., and Cohen, R. C.: Satellite measurements of daily variations in soil NO_x emissions, *Geophys. Res. Lett.*, 32, L24812, doi:10.1029/2005GL024640, 2005.
- 15 Bertram, T. H., Thornton, J. A., Riedel, T. P., Middlebrook, A. M., Bahreini, R., Bates, T. S., Quinn, P. K., and Coffman, D. J.: Direct observations of N₂O₅ reactivity on ambient aerosol particles, *Geophys. Res. Lett.*, 36, L19803, doi:10.1029/2009GL040248, 2009.
- 20 Binkowski, F. S. and Roselle, S. J.: Models-3 Community Multi-scale Air Quality (CMAQ) model aerosol components: 1. model description, *J. Geophys. Res.*, 108, 4183, doi:10.1029/2001JD001409, 2003.
- Boersma, K. F., Eskes, H. J., Veefkind, J. P., Brinksma, E. J., van der A, R. J., Sneep, M., van den Oord, G. H. J., Levelt, P. F., Stammes, P., Gleason, J. F., and Bucsela, E. J.: Near-real time retrieval of tropospheric NO₂ from OMI, *Atmos. Chem. Phys.*, 7, 2103–2118, doi:10.5194/acp-7-2103-2007, 2007.
- 25 Boersma, K. F., Jacob, D. J., Trainic, M., Rudich, Y., DeSmedt, I., Dirksen, R., and Eskes, H. J.: Validation of urban NO₂ concentrations and their diurnal and seasonal variations observed from the SCIAMACHY and OMI sensors using in situ surface measurements in Israeli cities, *Atmos. Chem. Phys.*, 9, 3867–3879, doi:10.5194/acp-9-3867-2009, 2009.

**Tropospheric NO₂
columns over East
Asia**

K. M. Han et al.

Title Page

Abstract

Introduction

Conclusions

References

Tables

Figures



Back

Close

Full Screen / Esc

Printer-friendly Version

Interactive Discussion



- Boersma, K. F., Eskes, H. J., Dirksen, R. J., van der A, R. J., Veefkind, J. P., Stammes, P., Huijnen, V., Kleipool, Q. L., Sneep, M., Claas, J., Leitão, J., Richter, A., Zhou, Y., and Brunner, D.: An improved tropospheric NO₂ column retrieval algorithm for the Ozone Monitoring Instrument, *Atmos. Meas. Tech.*, 4, 1905–1928, doi:10.5194/amt-4-1905-2011, 2011.
- 5 Brown, S. S., Dibb, J. E., Stark, H., Aldener, M., Vozella, M., Whitlow, S., Williams, E. J., Lerner, B. M., Jakoubek, R., Middlebrook, A. M., DeGouw, J. A., Warneke, C., Goldan, P. D., Kuster, W. C., Angevine, W. M., Sueper, D. T., Quinn, P. K., Bates, T. S., Meagher, J. F., Fehsenfeld, F. C., and Ravishankara, A. R.: Nighttime removal of NO_x in the summer marine boundary layer, *Geophys. Res. Lett.*, 31, L07108, doi:10.1029/2004GL019412, 2004.
- 10 Brown, S. S., Ryerson, T. B., Wollny, A. G., Brock, C. A., Peltier, R., Sullivan, A. P., Weber, R. J., Dube, W. P., Trainer, M., Meagher, J. F., Fehsenfeld, F. C., and Ravishankara, A. R.: Variability in nocturnal nitrogen oxide processing and its role in regional air quality, *Science*, 311, 67–70, 2006.
- Brown, S. S., Dubé, W. P., Fuchs, H., Ryerson, T. B., Wollny, A. G., Brock, C. A., Bahreini, R., Middlebrook, A. M., Neuman, J. A., Atlas, E., Roberts, J. M., Osthoff, H. D., Trainer, M., Fehsenfeld, F. C., and Ravishankara, A. R.: Reactive uptake coefficients for N₂O₅ determined from aircraft measurements during the Second Texas Air Quality Study: comparison to current model parameterizations, *J. Geophys. Res.*, 114, D00F10, doi:10.1029/2008JD011679, 2009.
- 20 Browne, E. C. and Cohen, R. C.: Effects of biogenic nitrate chemistry on the NO_x lifetime in remote continental regions, *Atmos. Chem. Phys.*, 12, 11917–11932, doi:10.5194/acp-12-11917-2012, 2012.
- Browne, E. C., Min, K.-E., Wooldridge, P. J., Apel, E., Blake, D. R., Brune, W. H., Cantrell, C. A., Cubison, M. J., Diskin, G. S., Jimenez, J. L., Weinheimer, A. J., Wennberg, P. O., Wisthaler, A., and Cohen, R. C.: Observations of total RONO₂ over the boreal forest: NO_x sinks and HNO₃ sources, *Atmos. Chem. Phys.*, 13, 4543–4562, doi:10.5194/acp-13-4543-2013, 2013.
- 25 Butkovskaya, N. I., Kukui, A., Pouvesle, N., and Le Bras, G.: Formation of nitric acid in the gas-phase HO₂ + NO reaction: effects of temperature and water vapor, *J. Phys. Chem. A*, 109, 6509–6520, doi:10.1021/jp051534v, 2005.
- 30 Butkovskaya, N., Rayez, M.-T., Rayez, J.-C., Kukui, A., and Le Bras, G.: Water vapor effect on the HNO₃ yield in the HO₂ + NO reaction: experimental and theoretical evidence, *J. Phys. Chem. A*, 113, 11327–11342, doi:10.1021/jp811428p, 2009.

**Tropospheric NO₂
columns over East
Asia**

K. M. Han et al.

Title Page

Abstract

Introduction

Conclusions

References

Tables

Figures



Back

Close

Full Screen / Esc

Printer-friendly Version

Interactive Discussion



Butler, T. M., Taraborrelli, D., Brühl, C., Fischer, H., Harder, H., Martinez, M., Williams, J., Lawrence, M. G., and Lelieveld, J.: Improved simulation of isoprene oxidation chemistry with the ECHAM5/MESSy chemistry-climate model: lessons from the GABRIEL airborne field campaign, *Atmos. Chem. Phys.*, 8, 4529–4546, doi:10.5194/acp-8-4529-2008, 2008.

Byun, D. W. and Schere, K. L.: Review of the governing equations, computational algorithm, and other components of the Models-3 Community Multi-scale Air Quality (CMAQ) Modeling system, *Appl. Mech. Rev.*, 59, 51–77, 2006.

Carter, W. P. L.: Implementation of the SAPRC-99 Chemical Mechanism into the Models-3 Framework, United States Environmental Protection Agency, 2000.

Cofala, J., Bertok, I., Borken-Kleefeld, J., Heyes, C., Klimont, Z., Rafaj, P., Sander, R., Schöpp, W., and Amann, M.: Emissions of Air Pollutants for the World Energy Outlook 2012 Energy Scenarios, International Institute for Applied System Analysis (IIASA), A-2361, Laxenburg, Austria, 2012.

Davis, J. M., Bhave, P. V., and Foley, K. M.: Parameterization of N₂O₅ reaction probabilities on the surface of particles containing ammonium, sulfate, and nitrate, *Atmos. Chem. Phys.*, 8, 5295–5311, doi:10.5194/acp-8-5295-2008, 2008.

Dentener, F. J. and Crutzen, P. J.: Reaction of N₂O₅ on tropospheric aerosols: impact on the global distribution of NO_x, O₃, and OH levels, *J. Geophys. Res.*, 98, 7149–7163, 1993.

Emmons, L. K., Walters, S., Hess, P. G., Lamarque, J.-F., Pfister, G. G., Fillmore, D., Granier, C., Guenther, A., Kinnison, D., Laepple, T., Orlando, J., Tie, X., Tyndall, G., Wiedinmyer, C., Baughcum, S. L., and Kloster, S.: Description and evaluation of the Model for Ozone and Related chemical Tracers, version 4 (MOZART-4), *Geosci. Model Dev.*, 3, 43–67, doi:10.5194/gmd-3-43-2010, 2010.

Eskes, H. J. and Boersma, K. F.: Averaging kernels for DOAS total-column satellite retrievals, *Atmos. Chem. Phys.*, 3, 1285–1291, doi:10.5194/acp-3-1285-2003, 2003.

Evans, M. J. and Jacob, D. J.: Impact of new laboratory studies of N₂O₅ hydrolysis on global model budgets of tropospheric nitrogen oxides, ozone, and OH, *Geophys. Res. Lett.*, 32, L09813, doi:10.1029/2005GL022469, 2005.

Fu, T., Jacob, D. J., Palmer, P. I., Chance, K., Wang, Y. X., Barletta, B., Blake, D. R., Stanton, J. C., and Pilling, M. J.: Space-based formaldehyde measurements as constrains on volatile organic compound emissions in east and south Asia and implications for ozone, *J. Geophys. Res.*, 112, D06312, doi:10.1029/2006JD007853, 2007.

**Tropospheric NO₂
columns over East
Asia**

K. M. Han et al.

Title Page

Abstract

Introduction

Conclusions

References

Tables

Figures



Back

Close

Full Screen / Esc

Printer-friendly Version

Interactive Discussion



- Ghude, Sachin, D., Pfister, Gabriele, G., Jena, Chinmay, van der A, R. J., Emmons, Louisa, K., and Kumar, Rajesh: satellite constraints of nitrogen oxide (NO_x) emissions from India based on OMI observations and WRF-Chem simulations, *Geophys. Res. Lett.*, 40, 1–6, doi:10.1029/2012GL053926, 2013.
- 5 Han, K. M. and Song, C. H.: A budget analysis of NO_x column losses over the Korean peninsula, *Asia-Pac. J. Atmos. Sci.*, 48, 55–65, 2012.
- Han, K. M., Song, C. H., Ahn, H. J., Park, R. S., Woo, J. H., Lee, C. K., Richter, A., Burrows, J. P., Kim, J. Y., and Hong, J. H.: Investigation of NO_x emissions and NO_x-related chemistry in East Asia using CMAQ-predicted and GOME-derived NO₂ columns, *Atmos. Chem. Phys.*, 9, 1017–1036, doi:10.5194/acp-9-1017-2009, 2009.
- 10 Han, K. M., Lee, C. K., Lee, J., Kim, J., and Song, C. H.: A comparison study between model-predicted and OMI-retrieved tropospheric NO₂ columns over the Korean peninsula, *Atmos. Environ.*, 45, 2962–2971, 2011.
- Han, K. M., Park, R. S., Kim, H. K., Woo, J. H., Kim, J., and Song, C. H.: Uncertainty in biogenic isoprene emissions and its impacts on tropospheric chemistry in East Asia, *Sci. Total Environ.*, 15 463, 754–771, 2013.
- Harris, G. W., Carter, W. P. L., Winer, A. M., Pitts, J. N., Platt, U., and Perner, D.: Observations of nitrous acid in the Los Angeles atmosphere and implications for predictions of ozone-precursor relationships, *Environ. Sci. Technol.*, 16, 414–419, doi:10.1021/es00101a009, 1982.
- 20 He, Y., Uno, I., Wang, Z., Ohara, T., Sugimoto, N., Shimizu, A., Richter, A., and Burrows, J. P.: Variations of the increasing trend of tropospheric NO₂ over central east China during the past decade, *Atmos. Environ.*, 41, 4865–4876, 2007.
- Henderson, B. H., Pinder, R. W., Crooks, J., Cohen, R. C., Carlton, A. G., Pye, H. O. T., and Vizuete, W.: Combining Bayesian methods and aircraft observations to constrain the HO[•] + NO₂ reaction rate, *Atmos. Chem. Phys.*, 12, 653–667, doi:10.5194/acp-12-653-2012, 2012.
- 25 Herron-Thorpe, F. L., Lamb, B. K., Mount, G. H., and Vaughan, J. K.: Evaluation of a regional air quality forecast model for tropospheric NO₂ columns using the OMI/Aura satellite tropospheric NO₂ product, *Atmos. Chem. Phys.*, 10, 8839–8854, doi:10.5194/acp-10-8839-2010, 2010.
- 30 Hong, J. H., Lee, W. S., Kim, D. G., Lee, S. B., and Kang, K. H.: 2006 Greenhouse Gas and Air Pollutants Emissions in Korea, National Institute of Environmental Research (NIER), Ministry of Environment of Korea, 2008.

**Tropospheric NO₂
columns over East
Asia**

K. M. Han et al.

Title Page

Abstract

Introduction

Conclusions

References

Tables

Figures



Back

Close

Full Screen / Esc

Printer-friendly Version

Interactive Discussion



- Horowitz, L., Fiore, A. M., Milly, G. P., Cohen, R. C., Perring, A., Wooldridge, P. J., Hess, P. G., Emmons, L. K., and Lamarque, J.-F.: Observational constraints on the chemistry of isoprene nitrates over the eastern United States, *J. Geophys. Res.*, 112, D12S08, doi:10.1029/2006JD007747, 2007.
- 5 Hudman, R. C., Russell, A. R., Valin, L. C., and Cohen, R. C.: Interannual variability in soil nitric oxide emissions over the United States as viewed from space, *Atmos. Chem. Phys.*, 10, 9943–9952, doi:10.5194/acp-10-9943-2010, 2010.
- Itahashi, S., Uno, I., Irie, H., Kurokawa, J.-I., and Ohara, T.: Regional modeling of tropospheric NO₂ vertical column density over East Asia during the period 2000–2010: comparison with multisatellite observations, *Atmos. Chem. Phys.*, 14, 3623–3635, doi:10.5194/acp-14-3623-2014, 2014.
- 10 Jacob, D. J.: Heterogeneous chemistry and tropospheric ozone, *Atmos. Environ.*, 34, 2131–2159, 2000.
- Jaeglé, L., Steinberger, L., Martin, R. V., and Chance, K.: Global partitioning of NO_x sources using satellite observations: relative roles of fossil fuel combustion, biomass burning and soil emissions, *Faraday Discuss.*, 130, 407–423, doi:10.1039/b502128f, 2005.
- Kim, J.: GEMS (Geostationary Environment Monitoring Spectrometer) onboard the GeoKOMP-SAT to Monitor Air Quality in high Temporal and Spatial Resolution over Asia-Pacific Region, EGU General Assembly 2012, 22–27 April 2012, Vienna, Austria, pp. 4051, 2012.
- 20 Klimont, Z., Cofala, J., Xing, J., Wei, W., Zhang, C., Wang, S., Kejun, J., Bhandari, P., Mathur, R., Purohit, P., Rafaj, P., Chambers, A., Amann, M., and Hao, J.: Projections of SO₂, NO_x, and carbonaceous aerosols emissions in Asia, *Tellus B*, 61, 602–617, 2009.
- Kubistin, D., Harder, H., Martinez, M., Rudolf, M., Sander, R., Bozem, H., Eerdekens, G., Fischer, H., Gurk, C., Klüpfel, T., Königstedt, R., Parchatka, U., Schiller, C. L., Stickler, A., Taraborrelli, D., Williams, J., and Lelieveld, J.: Hydroxyl radicals in the tropical troposphere over the Suriname rainforest: comparison of measurements with the box model MECCA, *Atmos. Chem. Phys.*, 10, 9705–9728, doi:10.5194/acp-10-9705-2010, 2010.
- 25 Kurokawa, J., Ohara, T., Morikawa, T., Hanayama, S., Janssens-Maenhout, G., Fukui, T., Kawashima, K., and Akimoto, H.: Emissions of air pollutants and greenhouse gases over Asian regions during 2000–2008: Regional Emission inventory in ASia (REAS) version 2, *Atmos. Chem. Phys.*, 13, 11019–11058, doi:10.5194/acp-13-11019-2013, 2013.
- 30 Lamsal, L. N., Martin, R. V., van Donkelaar, A., Celarier, E. A., Bucsela, E. J., Boersma, K. F., Dirksen, R., Luo, C., and Wang, Y.: Indirect validation of tropospheric nitrogen dioxide re-

**Tropospheric NO₂
columns over East
Asia**

K. M. Han et al.

Title Page

Abstract

Introduction

Conclusions

References

Tables

Figures



Back

Close

Full Screen / Esc

Printer-friendly Version

Interactive Discussion



trieved from the OMI satellite instrument: insight into the seasonal variation of nitrogen oxides at northern midlatitudes, *J. Geophys. Res.*, 115, D05302, doi:10.1029/2009JD013351, 2010.

Lelieveld, J., Butler, T. M., Crowley, J. N., Dillon, T. J., Fischer, H., Ganzeveld, L., Harder, H., Lawrence, M. G., Martinez, M., Taraborrelli, D., and Williams, J.: Atmospheric oxidation capacity sustained by a tropical forest, *Nature*, 452, 737–740, doi:10.1038/nature06870, 2008.

Levelt, P. F., van den Oord, G. H. J., Dobber, M. R., Mälkki, A., Visser, H., de Vries, J., Stammes, P., Lundell, J. O. V., and Saari, H.: The Ozone Monitoring Instrument, *IEEE T. Geosci. Remote*, 44, 1093–1101, 2006.

Lin, J.-T.: Satellite constraint for emissions of nitrogen oxides from anthropogenic, lightning and soil sources over East China on a high-resolution grid, *Atmos. Chem. Phys.*, 12, 2881–2898, doi:10.5194/acp-12-2881-2012, 2012.

Lin, J.-T., McElroy, M. B., and Boersma, K. F.: Constraint of anthropogenic NO_x emissions in China from different sectors: a new methodology using multiple satellite retrievals, *Atmos. Chem. Phys.*, 10, 63–78, doi:10.5194/acp-10-63-2010, 2010.

Lin, J.-T., Liu, Z., Zhang, Q., Liu, H., Mao, J., and Zhuang, G.: Modeling uncertainties for tropospheric nitrogen dioxide columns affecting satellite-based inverse modeling of nitrogen oxides emissions, *Atmos. Chem. Phys.*, 12, 12255–12275, doi:10.5194/acp-12-12255-2012, 2012.

Ma, J., Richter, A., Burrows, J. P., Nüß, H., and van Aardenne, J. A.: Comparison of model-simulated tropospheric NO₂ over China with GOME-satellite data, *Atmos. Environ.*, 40, 593–604, 2006.

Martin, R. V., Sioris, C. E., Chance, K., Ryerson, T. B., Bertram, T. H., Wooldridge, P. J., Cohen, R. C., Neuman, J. A., Swanson, A., and Flocke, F. M.: Evaluation of space-based constraints on global nitrogen oxide emissions with regional aircraft measurements over and downwind of eastern North America, *J. Geophys. Res.*, 111, D15308, doi:10.1029/2005JD006680, 2006.

Mijling, B., van der A, R. J., and Zhang, Q.: Regional nitrogen oxides emission trends in East Asia observed from space, *Atmos. Chem. Phys.*, 13, 12003–12012, doi:10.5194/acp-13-12003-2013, 2013.

Mollner, A. K., Valluvadasan, S., Feng, L., Sprague, M. K., Okumura, M., Milligan, D. B., Bloss, W. J., Sander, S. P., Martien, P. T., Harley, R. A., McCoy, A. B., and Carter, W. P. L.:

**Tropospheric NO₂
columns over East
Asia**

K. M. Han et al.

Title Page

Abstract

Introduction

Conclusions

References

Tables

Figures



Back

Close

Full Screen / Esc

Printer-friendly Version

Interactive Discussion



Rate of gas phase association of hydroxyl radical and nitrogen dioxide, *Science*, 330, 646–649, doi:10.1126/science.1193030, 2010.

Müller, J.-F., Stavrou, T., Wallens, S., De Smedt, I., Van Roozendael, M., Potosnak, M. J., Rinne, J., Munger, B., Goldstein, A., and Guenther, A. B.: Global isoprene emissions estimated using MEGAN, ECMWF analyses and a detailed canopy environment model, *Atmos. Chem. Phys.*, 8, 1329–1341, doi:10.5194/acp-8-1329-2008, 2008.

Ohara, T., Akimoto, H., Kurokawa, J., Horii, N., Yamaji, K., Yan, X., and Hayasaka, T.: An Asian emission inventory of anthropogenic emission sources for the period 1980–2020, *Atmos. Chem. Phys.*, 7, 4419–4444, doi:10.5194/acp-7-4419-2007, 2007.

Pagsberg, P., Bjergbakke, E., Ratajczak, E., and Sillescu, A.: Kinetics of the gas phase reaction $\text{OH} + \text{NO}(+\text{M}) \rightarrow \text{HONO}(+\text{M})$ and the determination of the UV absorption cross sections of HONO, *Chem. Phys. Lett.*, 272, 383–390, 1997.

Park, R. S., Han, K. M., Song, C. H., Park, M. E., Lee, S. J., Hong, S. Y., Kim, J., and Woo, J.-H.: Current status and development of modeling techniques for forecasting and monitoring of air quality over East Asia, *J. KOSAE*, 29, 407–438, 2013 (in Korean).

Park, R. S., Lee, S., Shin, S.-K., and Song, C. H.: Contribution of ammonium nitrate to aerosol optical depth and direct radiative forcing by aerosols over East Asia, *Atmos. Chem. Phys.*, 14, 2185–2201, doi:10.5194/acp-14-2185-2014, 2014.

Pleim, J. E.: A combined local and nonlocal closure model for the atmospheric boundary layer, Part I: Model description and testing, *J. Appl. Meteorol. Clim.*, 46, 1383–1395, 2007.

Pugh, T. A. M., MacKenzie, A. R., Hewitt, C. N., Langford, B., Edwards, P. M., Furneaux, K. L., Heard, D. E., Hopkins, J. R., Jones, C. E., Karunaharan, A., Lee, J., Mills, G., Misztal, P., Moller, S., Monks, P. S., and Whalley, L. K.: Simulating atmospheric composition over a South-East Asian tropical rainforest: performance of a chemistry box model, *Atmos. Chem. Phys.*, 10, 279–298, doi:10.5194/acp-10-279-2010, 2010.

Richter, A., Burrows, J. P., Nüß, H., Granier, C., and Niemeier, U.: Increase in tropospheric nitrogen dioxide over China observed from space, *Nature*, 437, 129–132, 2005.

Riener, N., Vogel, H., Vogel, B., Schell, B., Ackermann, I., Kessler, C., and Hass, H.: Impact of the heterogeneous hydrolysis of N_2O_5 on chemistry and nitrate aerosol formation in the lower troposphere under photochemical conditions, *J. Geophys. Res.*, 108, 4144, doi:10.1029/2002JD002436, 2003.

**Tropospheric NO₂
columns over East
Asia**

K. M. Han et al.

Title Page

Abstract

Introduction

Conclusions

References

Tables

Figures



Back

Close

Full Screen / Esc

Printer-friendly Version

Interactive Discussion



Rodgers, C. D.: Inverse methods for atmospheric sounding: theory and practice, Series on Atmospheric, Oceanic and Planetary Physics – Vol. 2, World Scientific Publishing, Singapore, 43–63, 2000.

Rondon, A. and Sanhueza, E.: High HONO atmospheric concentrations during vegetation burning in the tropical savannah, *Tellus B*, 41, 474–477, doi:10.1111/j.1600-0889.1989.tb00323.x, 1989.

Sander, S. P., Abbatt, J., Barker, J. R., Burkholder, J. B., Friedl, R. R., Golden, D. M., Huie, R. E., Kolb, C. E., Kurylo, M. J., Moortgat, G. K., Orkin, V. L., and Wine, P. H.: Chemical Kinetics and Photochemical Data for Use in Atmospheric Studies, Evaluation number 17, NASA Panel for data evaluation, JPL Publication 10–6, Jet Propulsion Laboratory, Pasadena, available at: <http://jpldataeval.jpl.nasa.gov> (last access: 27 June 2014), 2011.

Shi, C., Fernando, Wang, Z., An, X., and Wu, Q.: Tropospheric NO₂ columns over East Central China: comparisons between SCIAMACHY measurements and nested CMAQ simulations, *Atmos. Environ.*, 42, 7165–7173, 2008.

Sörgel, M., Regelin, E., Bozem, H., Diesch, J.-M., Drewnick, F., Fischer, H., Harder, H., Held, A., Hosaynali-Beygi, Z., Martinez, M., and Zetzsch, C.: Quantification of the unknown HONO daytime source and its relation to NO₂, *Atmos. Chem. Phys.*, 11, 10433–10447, doi:10.5194/acp-11-10433-2011, 2011.

Stauffer, D. R. and Seaman, N. L.: Use of four-dimensional data assimilation in a limited-area mesoscale model, Part I: experiments with synoptic-scale data, *Mon. Weather Rev.*, 118, 1250–1277, 1990.

Stauffer, D. L. and Seaman, N. L., Multiscale four-dimensional data assimilation, *J. Appl. Meteorol.*, 33, 416–434, 1994.

Stavrakou, T., Müller, J.-F., Boersma, K. F., De Smedt, I., and van der A, R. J.: Assessing the distribution and growth rates of NO_x emission sources by inverting a 10-year record of NO₂ satellite columns, *Geophys. Res. Lett.*, 35, L10801, doi:10.1029/2008GL033521, 2008.

Stavrakou, T., Müller, J.-F., Boersma, K. F., van der A, R. J., Kurokawa, J., Ohara, T., and Zhang, Q.: Key chemical NO_x sink uncertainties and how they influence top-down emissions of nitrogen oxides, *Atmos. Chem. Phys.*, 13, 9057–9082, doi:10.5194/acp-13-9057-2013, 2013.

Stemmler, K., Ammann, M., Donders, C., Kleffmann, J., and George, C.: Photosensitized reduction of nitrogen dioxide on humic acid as a source of nitrous acid, *Nature*, 440, 195–198, doi:10.1038/nature04603, 2006.

Tropospheric NO₂ columns over East Asia

K. M. Han et al.

Title Page

Abstract

Introduction

Conclusions

References

Tables

Figures



Back

Close

Full Screen / Esc

Printer-friendly Version

Interactive Discussion



- Streets, D. G., Bond, T. C., Carmichael, G. R., Fernandes, S. D., Fu, Q., He, D., Klimont, Z., Nelson, S. M., Tsai, N. Y., Wang, M. Q., Woo, J.-H., and Yarber, K. F.: An inventory of gaseous and primary aerosol emissions in Asia in the year 2000, *J. Geophys. Res.*, 108, 8809, doi:10.1029/2002JD003093, 2003.
- 5 Svensson, R., Ljungström, E., and Lindqvist, O.: Kinetics of the reaction between nitrogen dioxide and water vapour, *Atmos. Environ.*, 21, 1529–1539, 1987.
- Tie, X., Emmons, L., Horowitz, L., Brasseur, G., Ridley, B., Atlas, E., Stround, C., Hess, P., Klonecki, A., Madronich, S., Talbot, R., and Dibb, J.: Effect of sulfate aerosol on tropospheric NO_x and ozone budgets: model simulations and TOPSE evidence, *J. Geophys. Res.*, 108, 8364, doi:10.1029/2001JD001508, 2003.
- 10 Uno, I., He, Y., Ohara, T., Yamaji, K., Kurokawa, J.-I., Katayama, M., Wang, Z., Noguchi, K., Hayashida, S., Richter, A., and Burrows, J. P.: Systematic analysis of interannual and seasonal variations of model-simulated tropospheric NO₂ in Asia and comparison with GOME-satellite data, *Atmos. Chem. Phys.*, 7, 1671–1681, doi:10.5194/acp-7-1671-2007, 2007.
- 15 van der A, R. J., Peters, D. H. M. U., Eskes, H., Boersma, K. F., Van Roozendaal, M., De Smedt, I., and Kelder, H. M., Detection of the trend and seasonal variation in tropospheric NO₂ over China, *J. Geophys. Res.*, 111, 27, doi:10.1029/2005JD006594, 2006.
- Wang, Y., McElory, M. B., Martin, R. V., Streets, D. G., Zhang, Q., and Fu, T.-M.: Seasonal variability of NO_x emissions over east China constrained by satellite observations: implications for combustion and microbial sources, *J. Geophys. Res.*, 112, D06301, doi:10.1029/2006JD007538, 2007.
- 20 Wild, O., Prather, M. J., and Akimoto, H.: Indirect long-term global radiative cooling from NO_x emissions, *Geophys. Res. Lett.*, 28, 1719–1722, 2001.
- Willmott, C. J.: On the validation of models, *Phys. Geogr.*, 2, 184–194, 1981.
- 25 Xing, J., Wang, S. X., Chatani, S., Zhang, C. Y., Wei, W., Hao, J. M., Klimont, Z., Cofala, J., and Amann, M.: Projections of air pollutant emissions and its impacts on regional air quality in China in 2020, *Atmos. Chem. Phys.*, 11, 3119–3136, doi:10.5194/acp-11-3119-2011, 2011.
- Yamartino, R. J.: Nonnegative, conserved scalar transport using grid-cell-centered, spectrally constrained Blackman cubics for applications on a variable-thickness mesh, *Mon. Weather Rev.*, 121, 753–763, 1993.
- 30 Zhang, Q., Streets, D. G., He, K., Wang, Y., Richter, A., Burrows, J. P., Uno, I., Jang, C. J., Chen, D., Yao, Z., and Lei, Y.: NO_x emission trends for China, 1995–2004:

the view from the ground and the view from space, J. Geophys. Res., 112, D22306, doi:10.1029/2007JD008684, 2007.

Zhang, Q., Streets, D. G., Carmichael, G. R., He, K. B., Huo, H., Kannari, A., Klimont, Z., Park, I. S., Reddy, S., Fu, J. S., Chen, D., Duan, L., Lei, Y., Wang, L. T., and Yao, Z. L.: Asian emissions in 2006 for the NASA INTEX-B mission, Atmos. Chem. Phys., 9, 5131–5153, doi:10.5194/acp-9-5131-2009, 2009.

Zhou, X., Zhang, N., TerAvest, M., Tang, D., Hou, J., Bertman, S., Alaghmand, M., Shepson, P. B., Carroll, M. A., Griffith, S., Dusanter, S., and Stevens, P. S.: Nitric acid photolysis on forest canopy surface as a source for tropospheric nitrous acid, Nat. Geosci., 4, 440–443, doi:10.1038/ngeo1164, 2011.

Tropospheric NO₂ columns over East Asia

K. M. Han et al.

Title Page

Abstract

Introduction

Conclusions

References

Tables

Figures



Back

Close

Full Screen / Esc

Printer-friendly Version

Interactive Discussion



Tropospheric NO₂ columns over East Asia

K. M. Han et al.

Table 1. Description of CMAQ model simulations conducted in this study.

Cases	Sensitivity test	Month	Description	Section
1	Base-case simulation	Jan–Dec	– Seasonal variation of NO _x emission from INTEX-B inventory for China – NO _x emissions from INTEX-B, CAPSS, and REAS inventories for China, Korea, and Japan, respectively – Parameterization of γ_{NO_2} from the combination of Riemer et al. (2003) and Evans and Jacob (2005)	Sect. 3.1
2	Seasonal variation of NO _x emission	Jan–Dec	– As case 1 except for seasonal variation of NO _x emission from Han et al. (2009) for China	Sect. 3.2.1
3	Emission strength	Jan	– As case 1 except for NO _x emissions from REAS inventory for China	Sect. 3.2.2
4	Reaction probability of N ₂ O ₅	Jan	– As case 1 except for the $\gamma_{\text{N}_2\text{O}_5}$ parameterizations from: i. Dentener and Crutzen (1993); ii. Riemer et al. (2003); iii. Davis et al. (2008); and iv. Brown et al. (2006)	Sect. 3.2.3

Title Page

Abstract

Introduction

Conclusions

References

Tables

Figures



Back

Close

Full Screen / Esc

Printer-friendly Version

Interactive Discussion



Tropospheric NO₂
columns over East
Asia

K. M. Han et al.

Title Page

Abstract

Introduction

Conclusions

References

Tables

Figures

◀

▶

◀

▶

Back

Close

Full Screen / Esc

Printer-friendly Version

Interactive Discussion



Table 2. Average tropospheric NO₂ columns, standard deviations, and the normalized mean error (NME) with and without the application of AKs for four seasons.

Region	Season	$n^{(1)}$	Ω_{CMAQ} (w/o AKs) ⁽²⁾	$\Omega_{\text{CMAQ,AK}}$ (w/ AKs) ⁽²⁾	Ω_{OMI} ⁽²⁾	NME (w/o AKs)	NME (w/ AKs)	
CEC	Spring	900	13.01	(6.76) ⁽³⁾	6.39 (4.00) ⁽³⁾	6.89 (4.07)	91.41	29.69
	Summer	900	7.41	(4.58)	2.60 (1.92)	5.29 (3.02)	54.38	53.56
	Fall	900	14.66	(7.79)	7.16 (5.11)	9.49 (5.89)	60.90	33.33
	Winter	900	22.45	(11.67)	11.04 (7.60)	14.18 (8.05)	61.67	32.07
CEC2	Spring	820	12.11	(6.14)	4.79 (4.23)	4.45 (3.98)	172.02	29.92
	Summer	820	6.85	(6.13)	2.31 (3.10)	3.02 (2.15)	127.76	40.44
	Fall	820	14.96	(7.26)	5.58 (4.57)	4.97 (3.97)	200.97	37.22
	Winter	820	23.67	(7.05)	11.24 (5.64)	8.49 (5.79)	178.66	42.24
SC	Spring	1125	5.21	(3.25)	1.16 (1.08)	2.20 (2.03)	139.60	50.67
	Summer	1124	2.77	(2.28)	0.76 (0.88)	1.77 (1.73)	63.39	58.09
	Fall	1125	5.52	(3.24)	1.27 (1.05)	2.20 (2.31)	153.15	45.03
	Winter	1125	11.15	(4.35)	3.20 (1.92)	3.24 (3.39)	246.90	36.54
SB	Spring	408	5.84	(3.42)	1.52 (1.13)	2.56 (1.55)	133.96	45.31
	Summer	420	3.04	(2.03)	0.78 (0.61)	2.14 (0.99)	58.70	63.75
	Fall	418	9.37	(5.90)	2.30 (1.80)	2.71 (2.15)	251.27	44.93
	Winter	403	17.40	(9.46)	5.25 (4.23)	3.43 (3.01)	407.98	72.02
SK	Spring	260	9.16	(6.08)	4.95 (3.83)	5.24 (3.74)	74.90	27.63
	Summer	260	7.29	(8.41)	3.06 (4.11)	3.41 (2.58)	118.86	44.88
	Fall	260	9.72	(7.61)	4.59 (4.15)	4.81 (3.62)	107.70	40.03
	Winter	260	13.95	(6.18)	6.85 (3.67)	6.68 (4.14)	110.10	30.09
JP1	Spring	204	5.46	(1.87)	2.03 (0.79)	3.58 (2.48)	59.58	45.30
	Summer	204	2.84	(1.22)	0.78 (0.35)	2.91 (1.98)	37.78	73.27
	Fall	204	4.95	(2.21)	1.92 (0.95)	3.57 (2.50)	44.87	48.22
	Winter	204	8.69	(2.57)	3.48 (1.47)	4.48 (3.07)	96.62	37.46
JP2	Spring	285	4.77	(3.59)	1.74 (1.81)	3.09 (2.96)	54.88	45.18
	Summer	286	3.12	(2.97)	0.86 (0.89)	2.64 (2.77)	34.58	67.49
	Fall	286	4.35	(3.66)	1.63 (1.69)	3.12 (3.17)	41.55	47.98
	Winter	279	6.52	(5.03)	2.58 (2.50)	3.92 (4.20)	68.05	42.01
Entire domain	Spring	15175	3.63	(4.92)	1.35 (2.42)	1.97 (2.43)	103.44	46.09
	Summer	15207	2.04	(3.36)	0.64 (1.35)	1.59 (1.72)	65.86	63.62
	Fall	15224	4.12	(5.83)	1.45 (2.76)	2.06 (3.05)	111.73	44.77
	Winter	14075	7.37	(8.83)	2.95 (4.55)	3.20 (4.79)	135.06	40.47

⁽¹⁾ The number of data; ⁽²⁾ Unit, $\times 10^{15}$ molecules cm^{-2} ; ⁽³⁾ Standard deviations of the distributions of tropospheric NO₂ columns

Table 3. Reaction probabilities of N₂O₅ onto aerosol surfaces.

References	Condensing medium	Reaction probability of N ₂ O ₅ ($\gamma_{N_2O_5}$)
Dentener and Crutzen (1993) ¹ (Scheme I Fig. 10a)	Aqueous particles	$\gamma_{N_2O_5} = 0.1$
Jacob (2000) ^{1,2}	Aqueous particles	$\gamma_{N_2O_5} = 0.1$ (Range: 0.01–1)
Tie et al. (2003) ¹	Aqueous particles	$\gamma_{N_2O_5} = 0.04$ (Range: 0.0–0.10)
Riemer et al. (2003) ¹ (Scheme II in Fig. 10b)	Sulfate and Nitrate	$\gamma_{N_2O_5} = f \times \gamma_1 + (1 - f) \times \gamma_2$ (Range: 0.02–0.002) $\gamma_1 = 0.02, \gamma_2 = 0.002; f = \frac{m_{SO_4^{2-}}}{m_{SO_4^{2-}} + m_{NO_3^-}}$ $m_{SO_4^{2-}}$ and $m_{NO_3^-}$: aerosol mass concentrations of sulfate and nitrate, respectively
Evans and Jacob (2005) ¹	Sulfate	$\gamma_{N_2O_5} = \alpha \times 10^\beta$ $\alpha = 2.79 \times 10^{-4} + 1.3 \times 10^{-4} \times RH - 3.43 \times 10^{-6} \times RH^2 + 7.52 \times 10^{-8} \times RH^3$ $\beta = 4 \times 10^{-2} \times (294 - T)$ ($T \geq 282$ K) $\beta = 0.48$ ($T < 282$ K)
	OC	$\gamma_{N_2O_5} = RH \times 5.2 \times 10^{-4}$ ($RH < 57\%$) $\gamma_{N_2O_5} = 0.03$ ($RH \geq 57\%$)
	BC	$\gamma_{N_2O_5} = 0.005$
	Sea salt	$\gamma_{N_2O_5} = 0.005$ ($RH < 62\%$) $\gamma_{N_2O_5} = 0.03$ ($RH \geq 62\%$)
	Dust	$\gamma_{N_2O_5} = 0.01$ RH : relative humidity (%); T : temperature (K)
Combination of parameterization by Evan and Jacob (2005) and Riemer et al. (2003) ¹ (Scheme III in Fig. 10c)	Sulfate and Nitrate	$\gamma_{N_2O_5} = f \cdot \gamma_1 + (1 - f) \cdot \gamma_2$ $\alpha = 2.79 \times 10^{-4} + 1.3 \times 10^{-4} \times RH - 3.43 \times 10^{-6} \times RH^2 + 7.52 \times 10^{-8} \times RH^3$ $f = \frac{m_{SO_4^{2-}}}{m_{SO_4^{2-}} + m_{NO_3^-}}$ $\gamma_1 = \alpha \times 10^{0.48T}$; $\gamma_2 = 0.1 \times \gamma_1$ ($T < 282$ K) $\gamma_1 = \alpha \times 10^\beta$; $\gamma_2 = 0.1 \times \gamma_1$; $\beta = 4 \times 10^{-2} \times (294 - T)$ ($T \geq 282$ K)
Davis et al. (2008) ¹ (Scheme IV in Fig. 10d)	Aqueous particles	$\gamma_{N_2O_5, \text{mix}} = \sum_{i=1}^3 x_i \cdot \gamma_i$ $x_1 = 1 - (x_2 + x_3)$ for bisulfate $x_2 = \max\left(0, \min\left(1 - x_3, \frac{c_{\text{Ammonio}}}{c_{\text{NH}_4^+} + c_{\text{Sulfate}}} - 1\right)\right)$ for sulfate $x_3 = \frac{c_{\text{Nitrate}}}{c_{\text{NH}_4^+} + c_{\text{Sulfate}}}$ for nitrate $\lambda_1 = -4.559088 + 2.8593 \times RH - 0.111201 \times T_{287}$; $\gamma_1 = \min\left(\frac{1}{1 + e^{-\lambda_1}}, 0.08585\right)$ $\lambda_2 = \lambda_1 - 0.369769$; $\gamma_2 = \min\left(\frac{1}{1 + e^{-\lambda_2}}, 0.053\right)$ $\lambda_3 = -0.8107744 + 4.9017 \times RH$; $\gamma_3 = \min\left(\frac{1}{1 + e^{-\lambda_3}}, 0.0154\right)$ c_{Ammonio} , $c_{\text{NH}_4^+}$, and c_{Sulfate} : molar concentration of ammonium, nitrate, and sulfate, respectively
	Dry particles	$\gamma_{N_2O_5, \text{mix}} = (x_1 + x_2) \gamma_d + x_3 \times \min(\gamma_d, \gamma_3)$ $\lambda_d = -6.133764 + 3.5920 \times RH - 0.196879 \times T_{293}$; $\gamma_d = \min\left(\frac{1}{1 + e^{-\lambda_d}}, 0.0124\right)$
Brown et al. (2006) ² (Scheme V in Fig. 10e)		$\gamma_{N_2O_5} = \frac{4k_{N_2O_5}}{c_{\text{mean}} A}$ (i) 0.017 ± 0.004 (over Ohio and western Pennsylvania, US) (ii) < 0.0010 (over eastern Pennsylvania and New Jersey, US) (iii) < 0.0016 (over New York, US) $k_{N_2O_5}$: rate constant (s ⁻¹); c_{mean} : mean molecular speed of N ₂ O ₅ (cm s ⁻¹); A : aerosol surface density (μm ² cm ⁻³)

¹ Modelling study; ² Measurement study.

Title Page

Abstract

Introduction

Conclusions

References

Tables

Figures



Back

Close

Full Screen / Esc

Printer-friendly Version

Interactive Discussion



Tropospheric NO₂
columns over East
Asia

K. M. Han et al.

Title Page

Abstract

Introduction

Conclusions

References

Tables

Figures



Back

Close

Full Screen / Esc

Printer-friendly Version

Interactive Discussion

**Table 4.** Average tropospheric NO₂ columns, standard deviations and the ratios of the $\Omega_{\text{NO}_2, \text{CMAQ, AK}}$ to the $\Omega_{\text{NO}_2, \text{OMI}}$, when different $\gamma_{\text{N}_2\text{O}_5}$ parameterizations were applied to the CMAQ model simulations for January.

Region	Scheme ⁽¹⁾	$n^{(2)}$	$\Omega_{\text{CMAQ, AK}}^{(3)}$	$\Omega_{\text{OMI}}^{(3)}$	$R = \Omega_{\text{CMAQ, AK}} / \Omega_{\text{OMI}}$
CEC	Scheme I	896	11.06 (8.55) ⁽⁴⁾	13.92 (9.04)	0.79
	Scheme II		12.35 (9.48)		0.89
	Scheme III		12.26 (9.41)		0.88
	Scheme IV		12.16 (9.34)		0.87
	Scheme V		14.18 (10.94)		1.02
CEC2	Scheme I	820	9.79 (6.24)	7.85 (6.26)	1.25
	Scheme II		11.38 (6.87)		1.45
	Scheme III		11.44 (6.92)		1.46
	Scheme IV		11.26 (6.84)		1.43
	Scheme V		13.55 (7.70)		1.73
SC	Scheme I	1124	2.46 (1.78)	2.92 (3.13)	0.84
	Scheme II		2.87 (1.92)		0.98
	Scheme III		2.79 (1.86)		0.96
	Scheme IV		2.76 (1.86)		0.95
	Scheme V		3.43 (2.10)		1.18
SB	Scheme I	383	5.03 (4.50)	3.34 (2.53)	1.51
	Scheme II		5.67 (4.91)		1.70
	Scheme III		5.42 (4.71)		1.62
	Scheme IV		5.42 (4.72)		1.62
	Scheme V		6.76 (5.73)		2.02
SK	Scheme I	260	6.83 (4.00)	6.82 (4.64)	1.00
	Scheme II		7.46 (4.12)		1.09
	Scheme III		7.32 (4.08)		1.07
	Scheme IV		7.30 (4.08)		1.07
	Scheme V		8.45 (4.31)		1.24
JP1	Scheme I	201	3.53 (1.92)	4.72 (2.95)	0.75
	Scheme II		3.97 (2.08)		0.84
	Scheme III		3.81 (2.03)		0.81
	Scheme IV		3.83 (2.03)		0.81
	Scheme V		4.35 (2.19)		0.92
JP2	Scheme I	180	2.84 (2.77)	5.08 (4.99)	0.56
	Scheme II		3.05 (2.91)		0.60
	Scheme III		2.97 (2.84)		0.58
	Scheme IV		2.98 (2.85)		0.59
	Scheme V		3.35 (3.04)		0.66
Entire domain	Scheme I	12767	2.89 (4.86)	3.23 (5.11)	0.90
	Scheme II		3.29 (5.44)		1.02
	Scheme III		3.24 (5.43)		1.00
	Scheme IV		3.21 (5.37)		1.00
	Scheme V		3.84 (6.27)		1.19

⁽¹⁾ Scheme I (Dentener and Crutzen, 1993), Scheme II (Riemer et al., 2003), Scheme III (combination of Riemer et al., 2003 and Evans and Jacob, 2005), Scheme IV (Davis et al., 2007), Scheme V (Brown et al., 2006); ⁽²⁾ The number of data; ⁽³⁾ Unit, $\times 10^{16}$ molecules cm^{-2} ; ⁽⁴⁾ Standard deviations of the distributions of tropospheric NO₂ columns.

Tropospheric NO₂
columns over East
Asia

K. M. Han et al.

Title Page

Abstract

Introduction

Conclusions

References

Tables

Figures



Back

Close

Full Screen / Esc

Printer-friendly Version

Interactive Discussion

**Table A1.** Statistical parameters used in this study.

Parameters (unit)	Equations *	Range
Mean Error (molecules cm ⁻²)	$ME = \frac{1}{N} \sum_{i=1}^N \Omega_{\text{NO}_2, \text{CMAQ, AK}} - \Omega_{\text{NO}_2, \text{OMI}} $	0 to +∞
Mean Bias (molecules cm ⁻²)	$MB = \frac{1}{N} \sum_{i=1}^N (\Omega_{\text{NO}_2, \text{CMAQ, AK}} - \Omega_{\text{NO}_2, \text{OMI}}) =$ $\frac{\Omega_{\text{NO}_2, \text{CMAQ, AK}} - \Omega_{\text{NO}_2, \text{OMI}}}{N}$	$-\overline{\Omega_{\text{NO}_2, \text{OMI}}}$ to +∞
Mean Normalized Gross Error (%)	$MNGE = \frac{1}{N} \sum_{i=1}^N \frac{ \Omega_{\text{NO}_2, \text{CMAQ, AK}} - \Omega_{\text{NO}_2, \text{OMI}} }{\Omega_{\text{NO}_2, \text{OMI}}} \times 100$	0 to +∞
Mean Normalized Bias (%)	$MNB = \frac{1}{N} \sum_{i=1}^N \left(\frac{\Omega_{\text{NO}_2, \text{CMAQ, AK}} - \Omega_{\text{NO}_2, \text{OMI}}}{\Omega_{\text{NO}_2, \text{OMI}}} \right) \times 100$	-100 to +∞
Normalized Mean Error (%)	$NME = \frac{\sum_{i=1}^N \Omega_{\text{NO}_2, \text{CMAQ, AK}} - \Omega_{\text{NO}_2, \text{OMI}} }{\sum_{i=1}^N \Omega_{\text{NO}_2, \text{OMI}}} \times 100$	0 to +∞
Normalized Mean Bias (%)	$NMB = \frac{\sum_{i=1}^N (\Omega_{\text{NO}_2, \text{CMAQ, AK}} - \Omega_{\text{NO}_2, \text{OMI}})}{\sum_{i=1}^N \Omega_{\text{NO}_2, \text{OMI}}} \times 100$	-100 to +∞
Mean Fractional Error (%)	$MFE = \frac{1}{N} \sum_{i=1}^N \frac{ \Omega_{\text{NO}_2, \text{CMAQ, AK}} - \Omega_{\text{NO}_2, \text{OMI}} }{\left(\frac{\Omega_{\text{NO}_2, \text{CMAQ, AK}} + \Omega_{\text{NO}_2, \text{OMI}}}{2} \right)} \times 100$	0 to +200
Mean Fractional Bias (%)	$MFB = \frac{1}{N} \sum_{i=1}^N \frac{(\Omega_{\text{NO}_2, \text{CMAQ, AK}} - \Omega_{\text{NO}_2, \text{OMI}})}{\left(\frac{\Omega_{\text{NO}_2, \text{CMAQ, AK}} + \Omega_{\text{NO}_2, \text{OMI}}}{2} \right)} \times 100$	-200 to +200
Pearson correlation coefficient (dimensionless)	$R = \frac{\sum_{i=1}^N (\Omega_{\text{NO}_2, \text{CMAQ, AK}} - \overline{\Omega_{\text{NO}_2, \text{CMAQ, AK}}})(\Omega_{\text{NO}_2, \text{OMI}} - \overline{\Omega_{\text{NO}_2, \text{OMI}}})}{\sqrt{\sum_{i=1}^N (\Omega_{\text{NO}_2, \text{CMAQ, AK}} - \overline{\Omega_{\text{NO}_2, \text{CMAQ, AK}}})^2 \sum_{i=1}^N (\Omega_{\text{NO}_2, \text{OMI}} - \overline{\Omega_{\text{NO}_2, \text{OMI}}})^2}}$	-1 to +1
Index of agreement (dimensionless)	$IOA = 1 - \frac{\sum_{i=1}^N (\Omega_{\text{NO}_2, \text{CMAQ, AK}} - \Omega_{\text{NO}_2, \text{OMI}})^2}{\sum_{i=1}^N (\Omega_{\text{NO}_2, \text{CMAQ, AK}} - \Omega_{\text{NO}_2, \text{OMI}} + \Omega_{\text{NO}_2, \text{OMI}} - \overline{\Omega_{\text{NO}_2, \text{OMI}}})^2}$	0 to +1

* $\Omega_{\text{NO}_2, \text{CMAQ, AK}}$ and $\Omega_{\text{NO}_2, \text{OMI}}$ indicate the CMAQ-calculated NO₂ columns with the consideration of AKs and the OMI-retrieved NO₂ columns, respectively. *N* represents the number of data samples.

Tropospheric NO₂ columns over East Asia

K. M. Han et al.

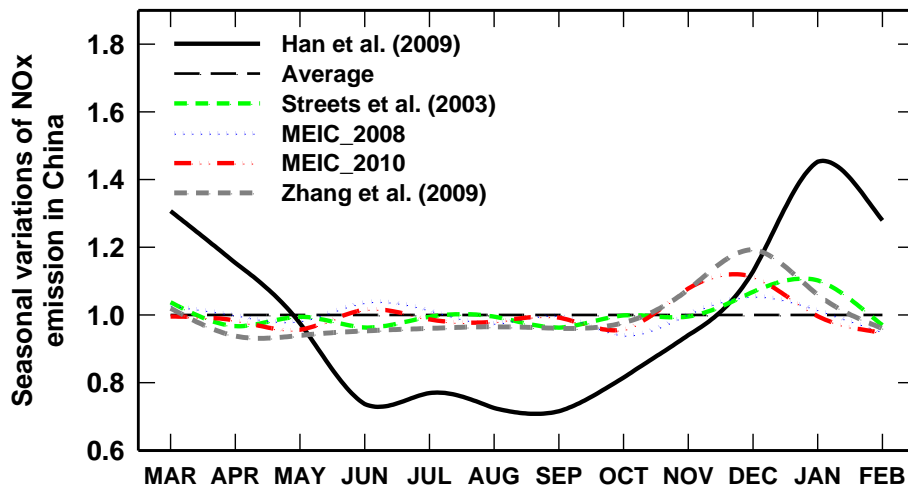


Figure 1. Monthly variation in NO_x emissions in China.

[Title Page](#)[Abstract](#)[Introduction](#)[Conclusions](#)[References](#)[Tables](#)[Figures](#)[Back](#)[Close](#)[Full Screen / Esc](#)[Printer-friendly Version](#)[Interactive Discussion](#)

Tropospheric NO₂ columns over East Asia

K. M. Han et al.

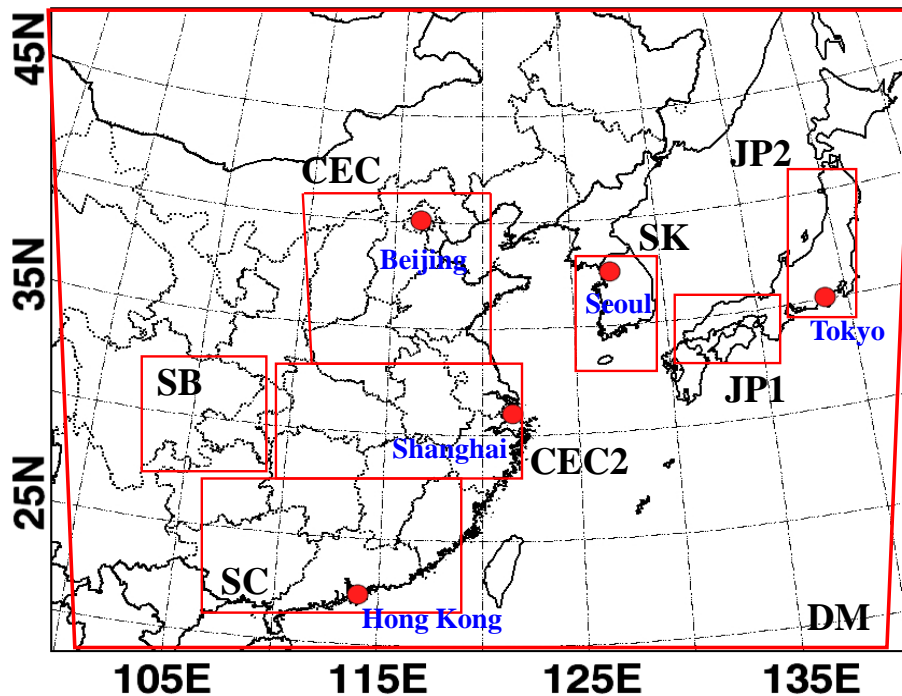


Figure 2. Study domain and eight focus regions in this study: central East China (CEC), Central East China 2 (CEC2), South China (SC), Sichuan Basin (SB), South Korea (SK), western part of Japan (JP1), eastern part of Japan (JP2), and entire domain (DM).

[Title Page](#)[Abstract](#)[Introduction](#)[Conclusions](#)[References](#)[Tables](#)[Figures](#)[◀](#)[▶](#)[◀](#)[▶](#)[Back](#)[Close](#)[Full Screen / Esc](#)[Printer-friendly Version](#)[Interactive Discussion](#)

Tropospheric NO₂
columns over East
Asia

K. M. Han et al.

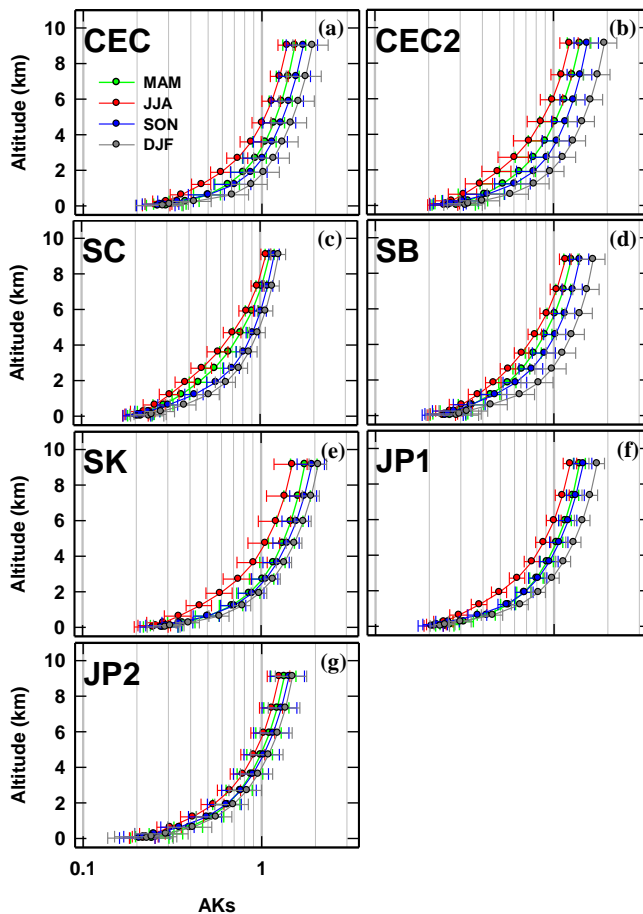


Figure 3. Vertical distributions of averaging kernels (AKs) for four seasons over (a) CEC, (b) CEC2, (c) SC, (d) SB, (e) SK, (f) JP1, and (g) JP2 regions.

[Title Page](#)[Abstract](#)[Introduction](#)[Conclusions](#)[References](#)[Tables](#)[Figures](#)[Back](#)[Close](#)[Full Screen / Esc](#)[Printer-friendly Version](#)[Interactive Discussion](#)

Tropospheric NO₂ columns over East Asia

K. M. Han et al.

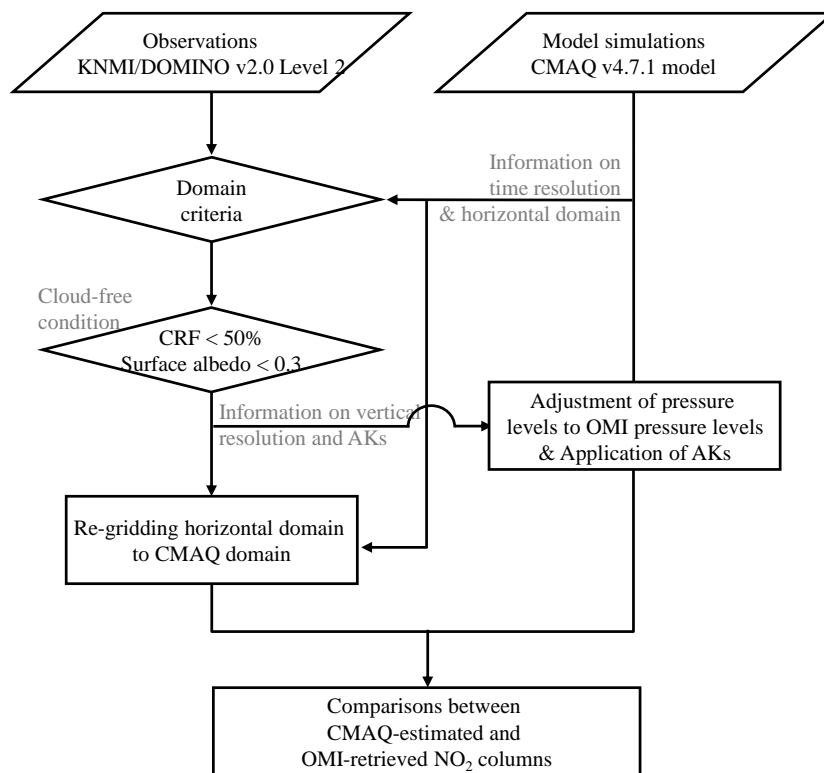


Figure 4. Flow diagram for direct comparison between CMAQ-estimated and OMI-retrieved NO₂ columns.

Title Page

Abstract

Introduction

Conclusions

References

Tables

Figures

◀

▶

◀

▶

Back

Close

Full Screen / Esc

Printer-friendly Version

Interactive Discussion



Tropospheric NO₂ columns over East Asia

K. M. Han et al.

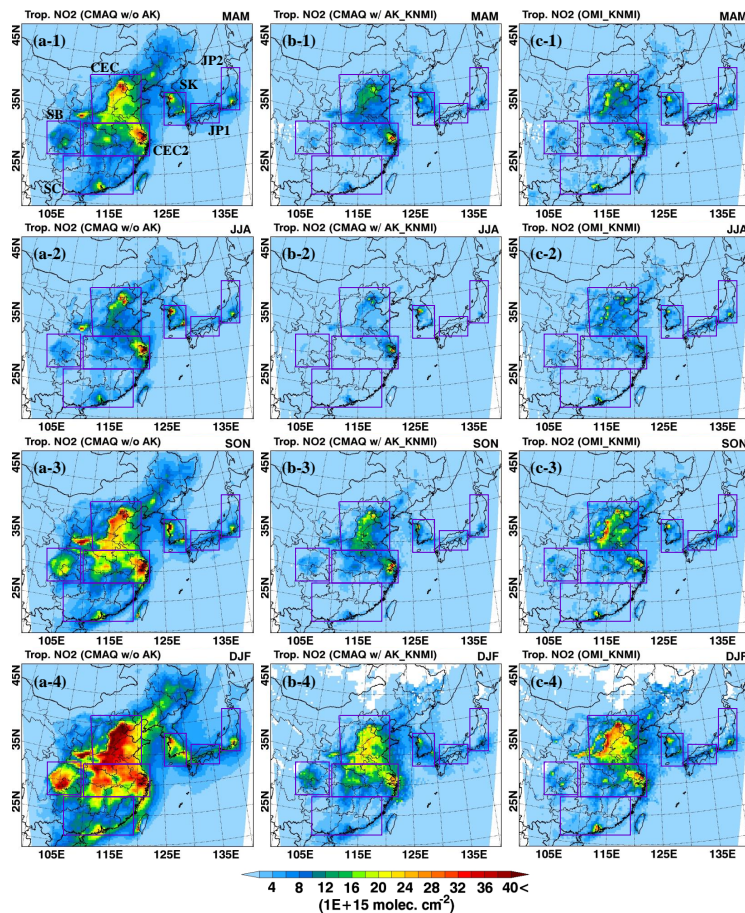


Figure 5. Spatial and seasonal distributions of CMAQ-calculated tropospheric NO₂ columns **(a)** without the applications of the AKs and **(b)** with the AKs and **(c)** OMI-retrieved NO₂ columns from the KNMI algorithm.

Tropospheric NO₂ columns over East Asia

K. M. Han et al.

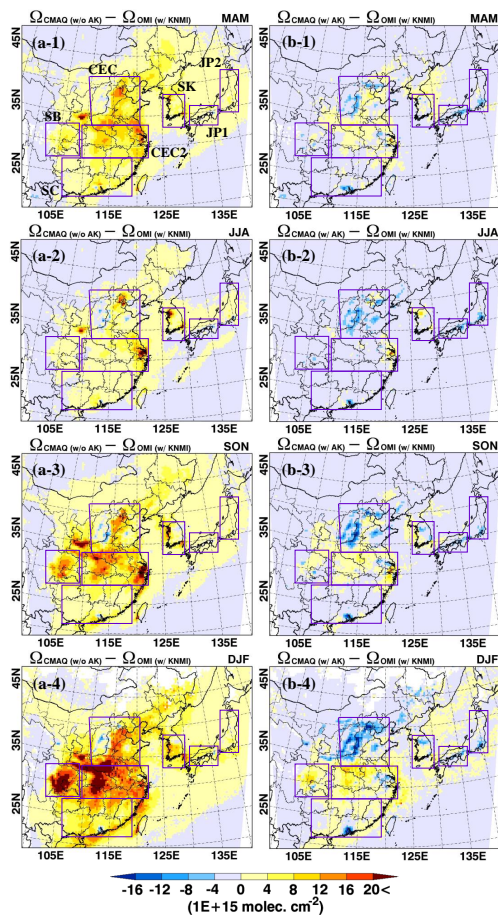


Figure 6. Differences between OMI-retrieved and CMAQ-calculated NO₂ columns **(a)** before the applications of the AKs and **(b)** after the applications of the AKs.

Title Page

Abstract

Introduction

Conclusions

References

Tables

Figures



Back

Close

Full Screen / Esc

Printer-friendly Version

Interactive Discussion



Tropospheric NO₂ columns over East Asia

K. M. Han et al.

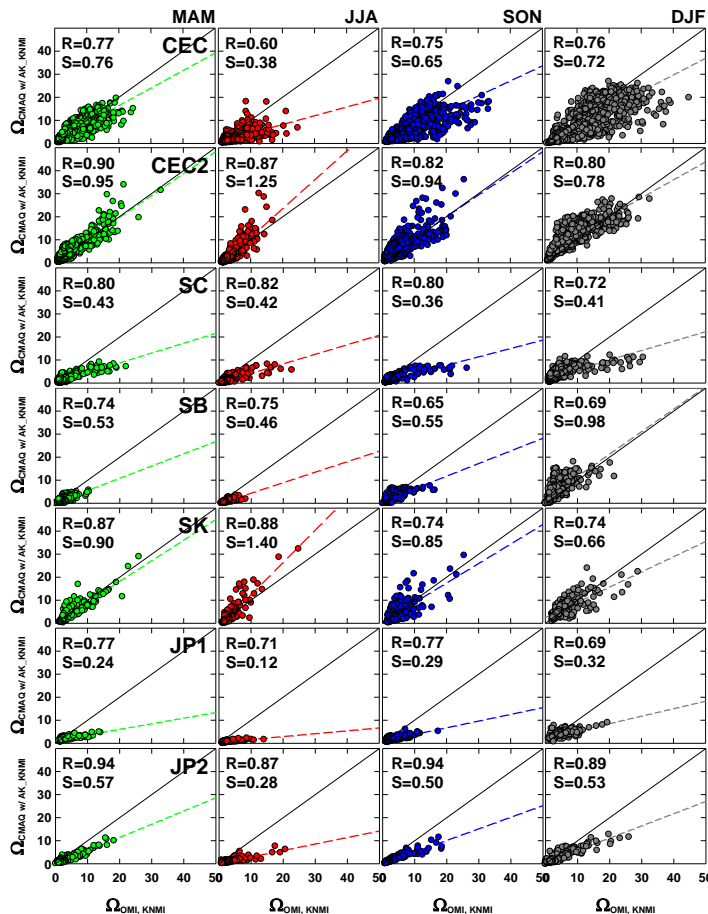


Figure 7. Seasonal scatter plots between CMAQ-calculated and OMI-retrieved NO₂ columns over the CEC, CEC2, SC, SB, SK, JP1, and JP2 regions. Here, the AKs were applied to the CMAQ model simulations.

Title Page

Abstract

Introduction

Conclusions

References

Tables

Figures

◀

▶

◀

▶

Back

Close

Full Screen / Esc

Printer-friendly Version

Interactive Discussion



Tropospheric NO₂ columns over East Asia

K. M. Han et al.

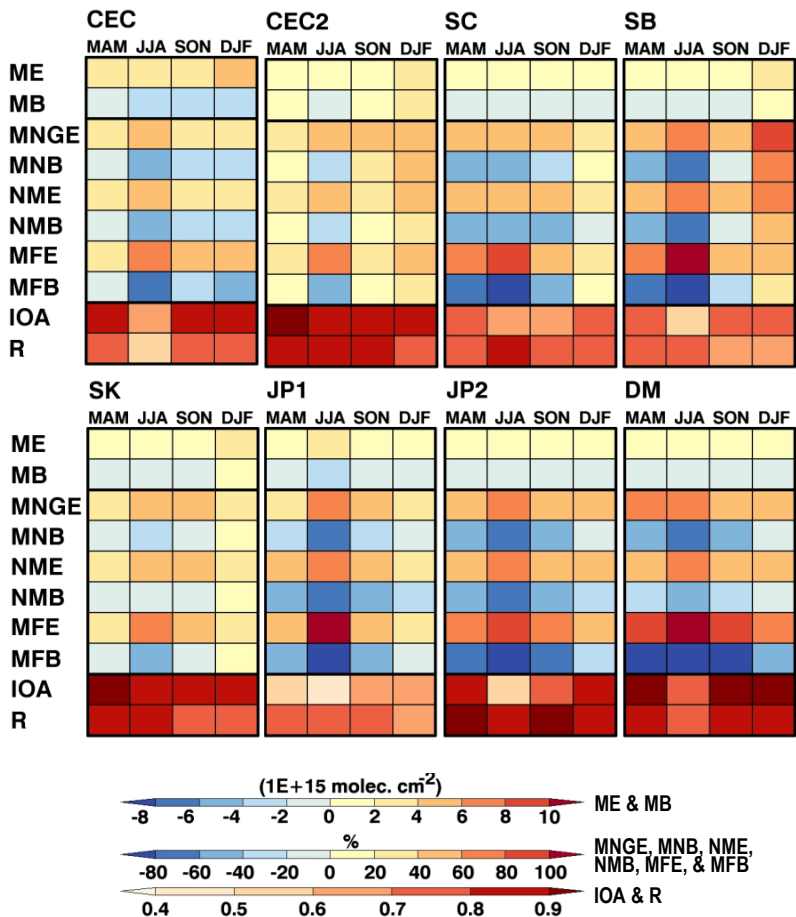


Figure 8. Statistical analyses between CMAQ-calculated and OMI-retrieved NO₂ columns using the performance metrics defined in Table A1. Here, the color bars represent ME and MB at the top, MNGE, MNB, NME, NMB, MFE, and MFB in the middle, and IOA and *R* at the bottom.

Title Page

Abstract Introduction

Conclusions References

Tables Figures

⏪ ⏩

◀ ▶

Back Close

Full Screen / Esc

Printer-friendly Version

Interactive Discussion



Tropospheric NO₂ columns over East Asia

K. M. Han et al.

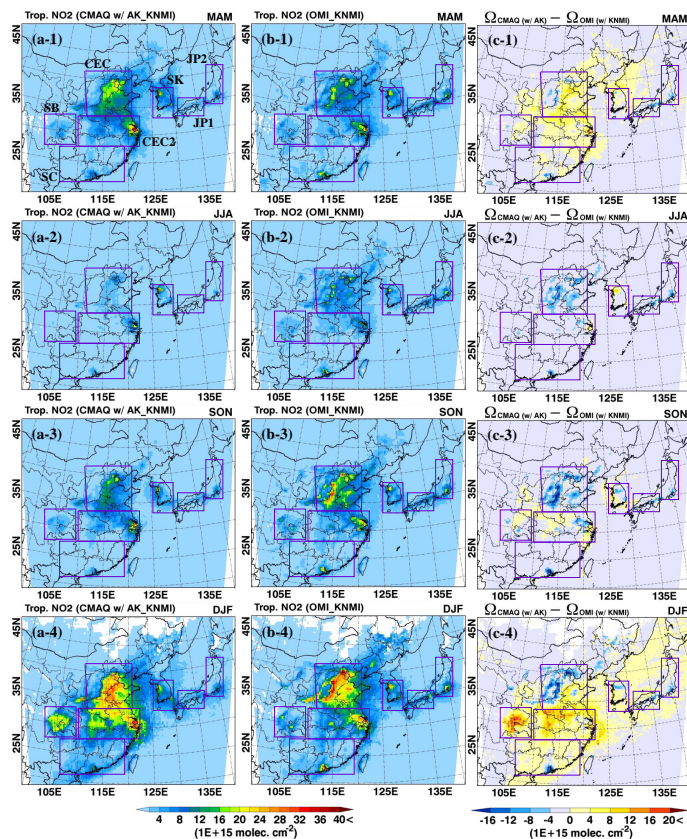


Figure 9. Spatial distributions of (a) CMAQ-calculated NO₂ columns with the AKs and (b) OMI-retrieved NO₂ columns and (c) their differences for four seasonal episodes. Here, the monthly variations of NO_x emissions from Han et al. (2009) were applied to the CMAQ model simulations.

Title Page

Abstract

Introduction

Conclusions

References

Tables

Figures



Back

Close

Full Screen / Esc

Printer-friendly Version

Interactive Discussion



Tropospheric NO₂
columns over East
Asia

K. M. Han et al.

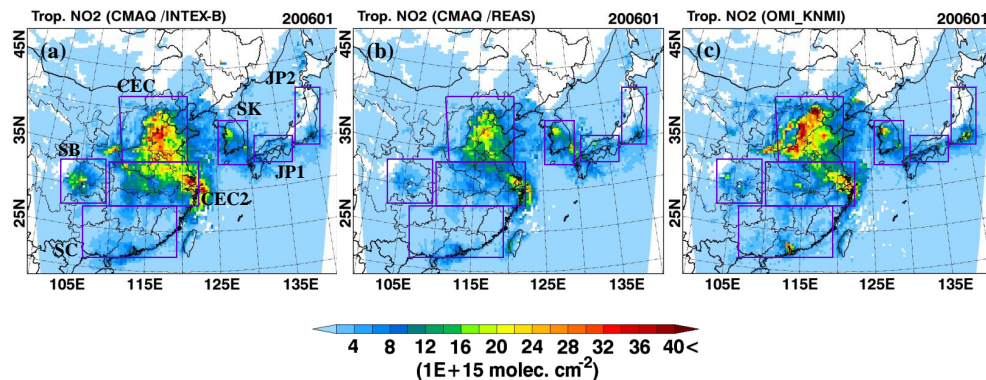


Figure 10. CMAQ-calculated NO₂ columns using (a) INTEX-B inventory and (b) REAS inventory over China and (c) OMI-observed NO₂ columns for January.

[Title Page](#)[Abstract](#)[Introduction](#)[Conclusions](#)[References](#)[Tables](#)[Figures](#)[◀](#)[▶](#)[◀](#)[▶](#)[Back](#)[Close](#)[Full Screen / Esc](#)[Printer-friendly Version](#)[Interactive Discussion](#)

Tropospheric NO₂
columns over East
Asia

K. M. Han et al.

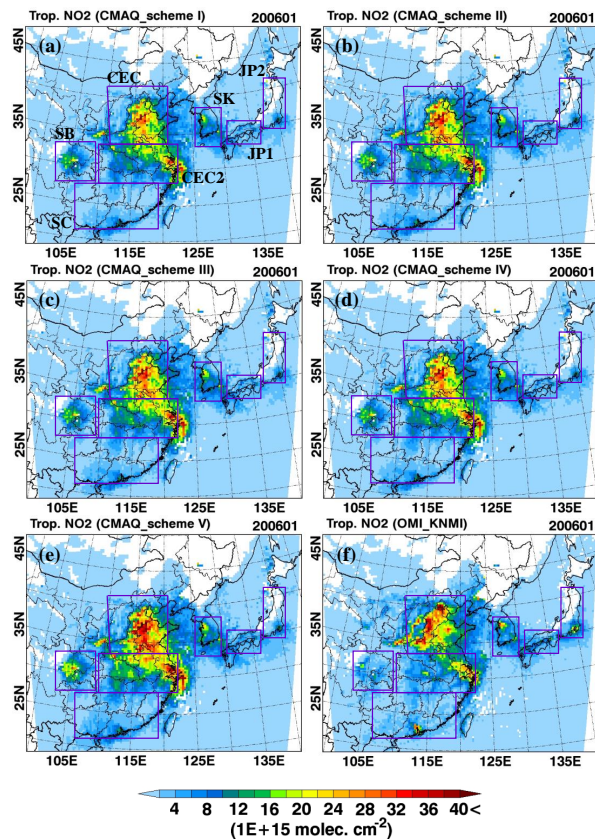


Figure 11. CMAQ-calculated NO₂ columns using five $\gamma_{\text{N}_2\text{O}_5}$ parameterizations from (a) Den- terner and Crutzen (1993), (b) Riemer et al. (2003), (c) combination of Riemer et al. (2003) and Evans and Jacob (2005), (d) Davis et al. (2008), and (e) Brown et al. (2006) and (f) OMI-observed NO₂ columns for January.

Title Page

Abstract

Introduction

Conclusions

References

Tables

Figures



Back

Close

Full Screen / Esc

Printer-friendly Version

Interactive Discussion

